2015

THE EFFECT OF CHOLESTEROL ON THE OSTEOBLAST RESPONSIVENESS TO HYDRODYNAMIC PRESSURE STIMULATION

Kristen Lough
University of Kentucky, knloug2@g.uky.edu

STUDENT AGREEMENT:

I represent that my thesis or dissertation and abstract are my original work. Proper attribution has been given to all outside sources. I understand that I am solely responsible for obtaining any needed copyright permissions. I have obtained needed written permission statement(s) from the owner(s) of each third-party copyrighted matter to be included in my work, allowing electronic distribution (if such use is not permitted by the fair use doctrine) which will be submitted to UKnowledge as Additional File.

I hereby grant to The University of Kentucky and its agents the irrevocable, non-exclusive, and royalty-free license to archive and make accessible my work in whole or in part in all forms of media, now or hereafter known. I agree that the document mentioned above may be made available immediately for worldwide access unless an embargo applies.

I retain all other ownership rights to the copyright of my work. I also retain the right to use in future works (such as articles or books) all or part of my work. I understand that I am free to register the copyright to my work.

REVIEW, APPROVAL AND ACCEPTANCE

The document mentioned above has been reviewed and accepted by the student's advisor, on behalf of the advisory committee, and by the Director of Graduate Studies (DGS), on behalf of the program; we verify that this is the final, approved version of the student's thesis including all changes required by the advisory committee. The undersigned agree to abide by the statements above.

Kristen Lough, Student

Dr. Hainsworth Y. Shin, Major Professor

Dr. Abhijit R. Patwardhan, Director of Graduate Studies

THE EFFECT OF CHOLESTEROL ON THE OSTEOBLAST RESPONSIVENESS TO HYDRODYNAMIC PRESSURE STIMULATION

THESIS

A thesis submitted in partial fulfillment of the requirements
for the degree of Master of Science in Biomedical Engineering
in the College of Engineering at the University of Kentucky

By

Kristen N. Lough

Director: Dr. Hainsworth Y. Shin, Professor of Biomedical Engineering

Lexington, Kentucky

2015

ABSTRACT OF THESIS

THE EFFECT OF CHOLESTEROL ON THE OSTEOBLAST RESPONSIVENESS TO HYDRODYNAMIC PRESSURE STIMULATION

Hypercholesterolemia is a risk factor for osteoporosis but the underlying mechanism is unknown. Previous evidence suggests that osteoporosis results from an impaired regulation of osteoblasts by fluid pressure fluctuations in the bone matrix. Recently, our laboratory showed that enhanced cholesterol in the cell membrane, due to hypercholesterolemia, alters leukocyte mechanosensitivity. We predict a similar link between osteoblasts and hypercholesterolemia leading to osteoporosis. Specifically, we hypothesize that extracellular cholesterol modifies the osteoblast sensitivity to pressure. MC3T3-E1 cells were exposed to hydrodynamic pressures regimes (mean=40mmHg, amplitude=0-20mmHg, frequency=1Hz) for 1-12 hours. To assess the impact of membrane cholesterol enrichment, cells were pre-treated with 0-50 μg/mL cyclodextran:cholesterol conjugates. We assessed the pressure effects on mitosis and F-actin stress fiber formation (SFF) of cells. Exposure of cells to 50/30 mmHg pressure transiently increased the number of cells in the S- and G_2M-phases of mitosis after 6 and 12 hours, respectively. Relative to controls, osteoblast-like cells exposed to all pressures exhibited significantly ($p<0.05$) enhanced SFF. The degree of SFF depended on the pressure amplitude and concentration of cyclodextran:cholesterol conjugates. Thus, enhanced membrane cholesterol alters the pressure sensitivity of osteoblasts. These data have implications as it relates to the negative impacts of hypercholesterolemia on bone physiology.

KEYWORDS: Osteoporosis, MC3T3, Hypercholesterolemia, Pressure, Mechanotransduction

Kristen N. Lough

January 14, 2015

THE EFFECT OF CHOLESTEROL ON THE OSTEOBLAST RESPONSIVENESS TO HYDRODYNAMIC PRESSURE STIMULATION

By

Kristen Lough

Hainsworth Y. Shin Ph.D.
Director of Thesis

Abhijit R. Patwardhan Ph.D.
Director of Graduate Studies

January 14, 2015

DEDICATION

I would like to dedicate this thesis to my supportive family, especially in living memory of my Uncle Dave Woeste, who inspired me to be "sharper than a marble".

ACKNOWLEDGMENTS

First, I would like to thank my advisor, Dr. Hainsworth Y. Shin, for his continuous support, guidance, motivation, enthusiasm, and patience throughout my research endeavors. Also, I would like to thank Dr. David Puleo and Dr. Babak Bazrgari for serving on my thesis committee. I would like to thank Dr. David Puleo for donating the MC3T3-E1 cells for my research studies too.

In addition, I would like to thank my enthusiastic lab mates including Dr. Bing Zhao, Dr. Xiaoyan Zhang, and Michael Akenhead for their tolerance and assistance in my research activities. Also, a thank you to Ryan Underwood for some additional figures.

I would like to thank the National Science Foundation-Kentucky EPSCoR Program- Bioengineering initiative and research scholars program and Biomedical Engineering Department at the University of Kentucky for their support during my research studies.

Finally, I would like to thank my family and friends, especially my parents for their continuous support and love while I chase my dreams.

Table of Contents

List of Tables

List of Figures

Introduction

Background of Osteoporosis

According to the National Osteoporosis Foundation and the National Institutes of Health, osteoporosis afflicts over 54 million Americans and is responsible for over 2 million broken bones per year [2, 3]. It is estimated that osteoporosis costs over $19 billion per year [2, 3]. By 2025, it is estimated that over 3 million osteoporotic fractures will occur, costing over $25 billion per year [2, 4]. An estimated 48 million people have low bone density, meaning 60% of adults over 50 are at risk of traumatic fractures [2, 4].

Osteoporosis is a silent disease of the bones caused by either increased bone resorption or reduced bone formation. These causes gradually reduce bone strength and quality leading to traumatic fractures. Recently, osteoporotic fractures have been shown to be the most common causes of disability and major medical costs in parts of the world[5]. Among osteoporotic patients, the hip and shoulder are the most common fractures [4]. Approximately 20% of older people who break a hip, die within one year from complications related to the fracture itself or the surgery to repair it [6]. Of those older people who survive osteoporotic fractures, many will need long-term nursing home care. Age is a significant risk factor of osteoporosis that is hard to treat which includes gender, ethnicity, family history, and a history of previous fractures [7, 8]. Also, there are many risk factors that can be improved through lifestyle choices which include physical activity, smoking, medications, body weight, and diet [7, 9, 10].

Dietary risks for osteoporosis have been largely attributed to a combination of lack of calcium and vitamin D deficiency [11]. Recently, however, human and animal studies have shown that high blood cholesterol is another risk factor for osteoporosis [12-16]. The link between elevated blood cholesterol levels and osteoporotic risk was suggested from observations of hypercholesterolemic patients who had been treated with statins, a cholesterol-lowering agent [17]. Once statin-use was implemented to reduce blood cholesterol levels in patients, osteoporosis risk was seen to be reduced [18]. In fact, statin-use increased the bone mass of hypercholesterolemic women and rats by increasing the bone metabolism [19-21]. Later studies [19-22] further supported the link between high blood cholesterol levels and osteoporosis.

Background of Hypercholesterolemia

Normal total cholesterol range for blood is between 140 and 200 mg/dL. High blood cholesterol levels, known as hypercholesterolemia, is a dominant risk factor for cardiovascular diseases that is largely attributed to the resultant development of chronic inflammation in the circulation [23, 24]. Hypercholesterolemia is characterized by blood plasma cholesterol concentrations greater than 240 mg/dL (6.2 mmol/L) [25].

Cholesterol is a fat-like substance stored in every cell in the human body. Cholesterol, in its free form, is most abundant in the cell membrane where it plays an important role in cell signaling processes including those of bone cells [26]. Notably, cholesterol levels in the cell membrane influence its fluidity and organization. Thus changes in membrane cholesterol content has been shown to influence signaling pathways in cells by its action on the fluidity of the lipid bilayer. In this way, altered

membrane cholesterol in cells such as the blood cells have been proposed to drive disease states.

The human body makes cholesterol naturally. Additional cholesterol comes from food that, when consumed in large quantities, evokes blood cholesterol elevations. This can lead to problems. For example, the traditional view is that elevated blood cholesterol causes fatty (atherosclerotic) plaque deposition along artery walls in the circulation which can eventually mature into large fatty lesions that may rupture resulting in the development of clots along the vessel wall. These clots can break off from the diseased vessel wall and turn into emboli that float downstream and block smaller vessels. In general, these blockages in coronary arteries lead to heart attacks or in the brain vasculature lead to stroke. In this way, hypercholesterolemia is thought to contribute to both cardiovascular disease and metabolic syndrome (obesity, type 2 diabetes, high blood pressure) [27-29].

But it is also possible that cholesterol causes cardiovascular disease by influencing the regulation of white blood cells by fluid shear stress mechanotransduction. Previously in our laboratory, it has been shown that hypercholesterolemia alters the mechanosensitivity of leukocytes, white blood cells, by altering the cholesterol related fluidity of the cell membrane [30]. This effect of hypercholesterolemia on leukocytes is thought to be associated with the pathogenesis of chronic inflammation in the blood that leads to cardiovascular disease. A similar mechanism with osteoblasts could possibly link osteoporosis and hypercholesterolemia.

Linking Osteoporotic Bone Remodeling and Hypercholesterolemia

Recently, hypercholesterolemia has been identified as a dominant risk factor for osteoporosis [31]. According to the National Health and Nutrition Examination Survey, 63% of osteoporotic patients have hyperlipidemia, i.e. a blood cholesterol concentration greater than 200 mg/dL [32]. The American Heart Association estimates that 34 million Americans have hypercholesterolemia, similar to the amount of people with low bone density [33]. It has been shown that hypercholesterolemic animals exhibit low bone density supposedly by blocking the differentiation of osteoblast progenitor cells and, in doing so, reducing bone mineralization [14, 16]. There is also evidence that osteoporosis due to high cholesterol diets results from an impairment of bone formation during the bone remodeling processes [15-19].

Cellular Basis for Mechanosensitivity Bone Remodeling

Physiological bone remodeling represents a balance between bone formation by osteoblasts and resorption by osteoclasts. As seen in Figure 1, normal bone remodeling is depicted with the osteoblasts, osteoclasts, and osteocytes.

Osteoblasts are the bone-forming cells, osteoclasts are the bone-resorbing cells, and osteocytes are the interconnected network of cell residing in the bone matrix (Figure 1). Osteocytes account for 90-95 % of bone cells and thus are thought to serve as the mechanosensory system for bone [34]. Typically, osteocytes are thought to be responsible for sensing changes of mechanical loading [35] in the bone which direct osteoclast and osteoblast movement and action. But, all three bone cell types have been shown to exhibit sensitivity to mechanical loading [34, 36].

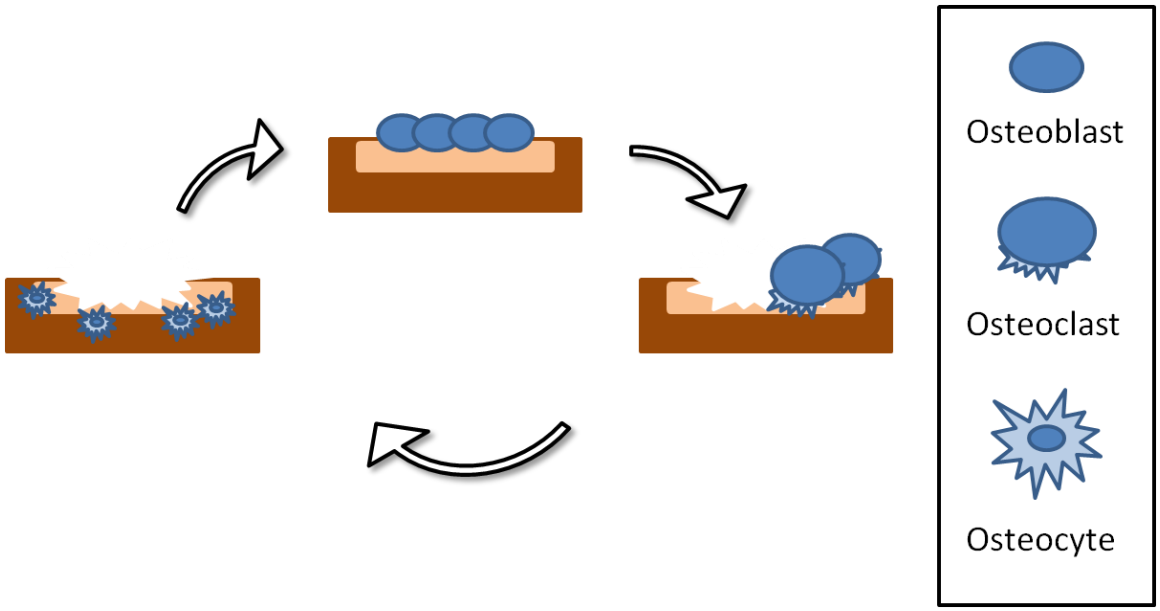

Figure 1: The Bone Remodeling Process with Osteoclasts, Osteoblasts, and Osteocytes. Three types of bone cells contribute to the bone remodeling process; osteoclasts are the bone-forming cells, osteoblasts are the bone-resorbing cells, and osteocytes line the bone matrix (adapted from [1]) .

A key principle that describes the regulation of the bone remodeling process is Wolff's law, which states that bone remodels its mineral content and structure in response to the imposed mechanical loading condition [37]. Reduced mechanical loading favors bone resorption leading to decreased bone density, whereas, enhanced loading favors bone formation leading to increased bone density. Osteoporosis is thought to result from an impairment in the mechanoregulation of the bone cells that leads to an imbalance between bone formation (osteoblasts) and resorption (osteoclasts).

The osteoblastic cellular response to mechanical stimuli such as fluid shear stress has been shown in previous studies [38]. But another way bone cells may sense dynamic loading is by the hydrodynamic pressures generated in the interstitial fluid of the bone matrix as a result of the force application [39-42]. Previous studies have shown that mechanical loading stimulates enhanced bone formation of osteoblasts in chick femurs and play an important role in the remodeling process in vivo [43].

Mechanosensitive Bone Remodeling

The mechanical stimuli induced on bone cells include strain, stress, pressure, interstitial fluid flow, and hydraulic pressure [38, 44-46]. Previous studies showed that bone cells can sense dynamic loading by hydrodynamic pressures transmitted to the interstitial fluid of the bone matrix [47-49]. The dynamic loading induces pressure fluctuations in the bone [38, 47-50]. Hydrodynamic pressures that mimic daily activities of cyclic loading (standing, walking, jogging) inhibit osteoclast activity [51-53] and stimulate osteoblast recruitment [39, 40, 42, 52, 54].

As shown in Figure 2, the mechanotransduction by osteoblasts involves a mechanical stimulus on the surface components (e.g. IGF, integrins, Wnt, and many more protein receptors) [37, 55]. In response to the changes in fluid stress levels from mechanical loading, cell surface components/mechanosensors are thought to undergo structural shifts which trigger downstream cell signaling pathways and functions (Figure 2) [37, 55]. Cytoskeletal changes and altered rates of mitosis [56, 57] represent some of the responses of osteoblasts to mechanical forces (Figure 2A). Fluid shear exposure of MC3T3 cells causes reorganization of their actin filaments and formation of parallel stress fibers [46, 58, 59]. Osteoblastic cells exposed to cyclic pressures also exhibit reorganization of f-actin networks [46]. Conceivably, the responses of osteoblasts to mechanical stresses such as hydrodynamic pressures derive from structural shifts of protein mechanosensors that span the cell membrane. It thus likely that through its influence on membrane fluidity, cholesterol may influence mechanosensitive osteoblast activity by affecting the ability of cell surface mechanosensors to undergo such conformational shifts (Figure 2B).

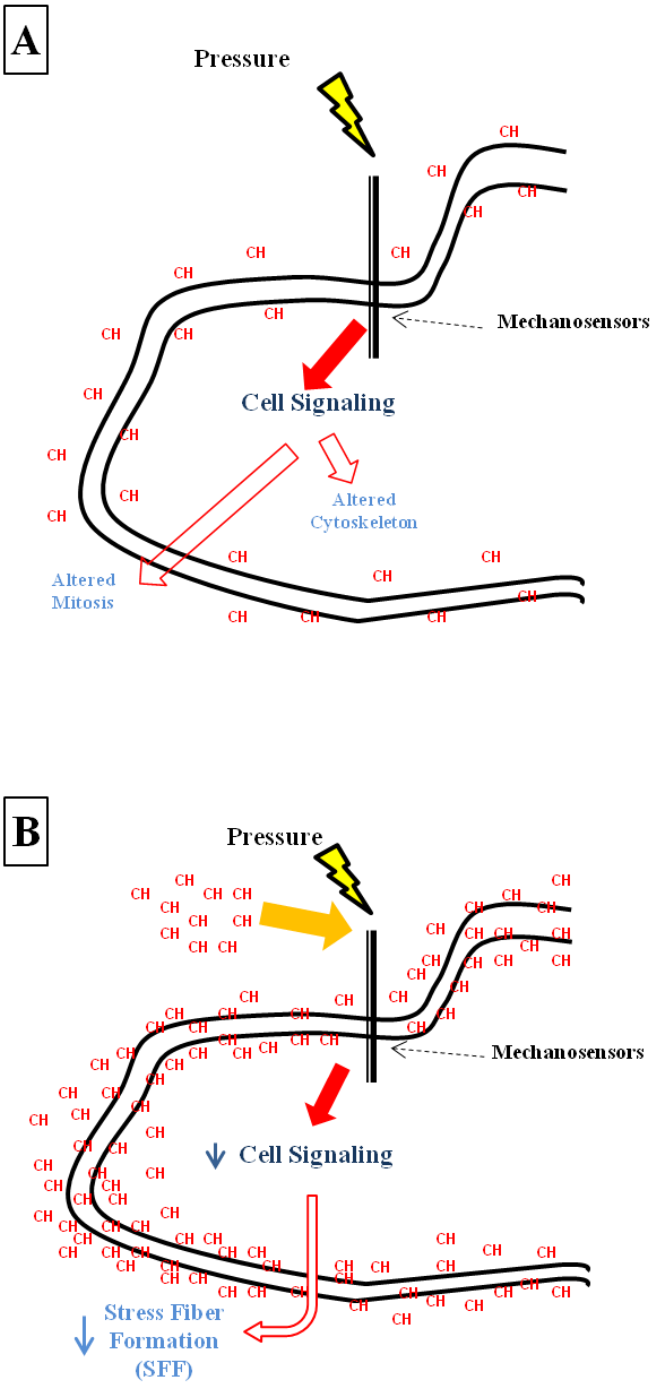

Figure 2: A Schematic Representing the Process of a Mechanical Stimulus Causing Changes in the Cell Membrane Through Mechanosensors Signaling Structural Shifts. [A] represents pressure stimulation on the cell membrane leading to an altered cell signaling pathway which alters the cell cytoskeleton and mitosis. [B] represents pressure stimulation on the cell membrane with additional cholesterol added which decreases cell signaling leading to decreased stress fiber formation (SFF). CH represents cholesterol conjugate. (Adapted from [60]).

Cholesterol Effects on Pressure-Sensitive Osteoblasts

Reportedly, cholesterol has been associated with the responses of osteoblasts to pressure since removal of this molecule from their membranes dampened pressure-related signaling [61]. It, however, is not known whether enrichment of the cell membrane with cholesterol, which may occur due to hypercholesterolemia, would also retard osteoblast responses. For example, it is possible that membrane cholesterol enrichment reduces the cell membrane fluidity, and in doing so, alters the pressure sensitivity of osteoblasts leading to altered bone formation activity, assuming deformation of mechanosensors on the cell surface drives pressure mechanotransduction. We propose such a pathogenic mechanism; specifically, an impaired mechanosensitivity of the osteoblasts to pressure stimuli is what underlies the link between osteoporosis and hypercholesterolemia. To establish this, we will to test the effects of membrane cholesterol enrichment and its impact on the membrane fluidity on the responsiveness of osteoblasts to pressure.

Rationale

Hypercholesterolemia has been identified as a risk factor for osteoporosis, a bone disease that afflicts millions of people. Osteoporosis results from deregulated bone remodeling consisting of an imbalance between the bone formation activity of osteoblasts and bone resorption by osteoclasts.

In healthy individuals, bone remodeling is widely accepted to be governed by Wolff's law that states bone remodels its microstructure and mineral content depending on its mechanical loading condition. This adaptive response at the tissue level is thought to arise from the bone cells whose activity has been shown to exhibit sensitivity to mechanical loading. One way that bone loading may influence the functions of bone cells is by inducing pressure fluctuations in their surrounding matrix. Previous studies have shown that bone cells are influenced by dynamic loading at the tissue level by the resulting hydrodynamic pressures generated in the interstitial fluid of the bone matrix [39-42, 51-54]. For example, it has been shown that exposure to osteoblastic cells to pressures up to 500 mmHg induce F-actin stress fiber formation [38].

Reportedly, osteoblast mechanotransduction of sustained hydrostatic pressure has been shown to depend on cholesterol compartments in the cell membrane [61]. Thus, changes in membrane cholesterol, such as during hypercholesterolemia, may contribute to an impairment in osteoblast mechanosensitivity that leads to their dysfunction. Recently, our laboratory showed for white blood cells that hypercholesterolemia alters their sensitivity to fluid stress stimulation by enhancing membrane cholesterol abundance [30]. We think hypercholesterolemia may also impair the pressure responses of osteoblasts. This may provide an explanation, at least in part, for the link between

hypercholesterolemia and osteoporosis. To address this possibility, we ran a series of pilot experiments to see if there is a connection between the responsiveness of osteoblasts to pressure and cholesterol enrichment of their cell membrane, which may occur due to hypercholesterolemia. Specifically, we tested the hypothesis that extracellular cholesterol levels influence the osteoblast mechanosensitivity to fluid pressure via its impact on the cell membrane. The goal of this study is to shed novel insight on a new potential link that could explain the relationship between hypercholesterolemia and osteoporosis. To address the hypothesis, we completed the three aims as follows.

1. Develop a MC3T3 cell culture model
2. Establish a hydrodynamic pressure system that imposes static and cyclic pressures on the MC3T3 cells
3. Identify the impact of cholesterol on hydrodynamic pressure responses in MC3T3 cells

Methods and Materials

Cell Culture Substrates

The two-dimensional polystyrene culture surfaces of individual wells of 12-well tissue culture plates or 100x20 mm tissue culture petridishes were overlaid with sterile 0.2% gelatin (Sigma-Aldrich) in aqueous solution and incubated for at least 15 minutes. Prior to cell seeding, the gelatin solution was aspirated from the tissue culture surfaces and allowed to dry.

Preparation of Glass Coverslips

Borosilicate glass coverslips (No. 1; Fisher Scientific®) were soaked in acetone for 10 minutes followed by sonication for 10 minutes. The coverslips were then rinsed of residual acetone by three washes in de-ionized water for 3-4 minutes each. They were then soaked in 70% ethanol for 10 minutes followed by sonication for 10 minutes. Residual ethanol was washed off the coverslips by three rinses in deionized water for 3-4 minutes each. Finally, the coverslips were pre-etched in 1M NaOH in de-ionized water for 1 hour. The coverslips were then thoroughly washed in de-ionized water for 3-4 minutes for at least three times. In preparation for sterilization, each coverslip was washed in de-ionized water individually before being placed in a glass petri-dish with Kim-wipe tissues (Kimberly Clark Professional) separating them from one another. The petri-dish with coverslips was subjected to steam autoclaving conditions (121^{o}C, 15 PSI) and then placed in a drying oven prior to use.

Cell Lines, Culture Conditions, and Passaging

MC3T3-E1 pre-osteoblastic cells were kindly provided by Dr. David Puleo from the Department of Biomedical Engineering at the University of Kentucky (Lexington, KY). MC3T3-E1 cells were cultured on gelatin-coated polystyrene surfaces in MEM Alpha Modification 1X Medium (HyClone®) supplemented with 10% v/v fetal bovine serum (FBS) (HyClone®) and 1% v/v penicillin/streptomycin/L-glutamine solution (HyClone®) under a humidified 5% carbon dioxide/95% air environment maintained at 37°C, i.e. standard incubator conditions.

For routine culture, the culture media was replaced every 2 to 3 days until cells reached confluence. At that time, MC3T3-E1 cultures were split (1:3 ratio) into new culture dishes. Briefly, cells were rinsed with PBS for 3 minutes and lifted by treatment with 0.5% trypsin/1 mM EDTA (Sigma) for 2 - 5 minutes. Following gentle agitation, cells were checked under the microscope to confirm their detachment from the culture dish. To remove the trypsin/EDTA solution, the detached cells were suspended in fresh media with serum and centrifuged at 200xG for 5 minutes at 25°C. After centrifugation, the supernatant solution was aspirated, and the resulting cell pellet was resuspended in fresh media and seeded in new tissue culture dishes. MC3T3-E1 cells of passages 8 to 20 were used in all experiments in the present study.

Cell Storage

Cryopreservation was used to store confluent MC3T3-E1 populations. MC3T3-E1 cells were washed with PBS for 5 minutes and lifted with 0.5% trypsin/1mM EDTA. The resulting cell suspension was combined with fresh media in a 15 mL centrifuge tube (BD Falcon®) and centrifuged at 200xG for 5 minutes at 25°C. The supernatant was aspirated,

and the resulting cell pellet was resuspended in 2 mL of freezing solution consisting of 10% dimethyl sulfoxide (DMSO) (Sigma®) in FBS, transferred to 2-mL cryogenic vials (BD Falcon), and stored in a -80°C freezer until needed or transferred to liquid-nitrogen for cryogenic storage.

When needed, frozen cells were rapidly thawed in a 37°C water bath. The thawed cell suspension was mixed with 5 mL of warm complete media in a 15-mL centrifuge tube and pelleted at 200xG for 5 minutes at 25°C. The cell pellet was resuspended in 10 mL complete media, transferred to a tissue culture dish, and cultured under standard cell culture conditions.

Cell Seeding

Seeding in Multi-Well Tissue Culture Plates

For analyses related to the pressure and cholesterol effects on the osteoblast cytoskeleton MC3T3-E1 cells were seeded on glass coverslips that had been placed in individual wells of a 12-well tissue culture polystyrene plate (BD Falcon®). Briefly, MC3T3-E1 cells were lifted using trypsin, centrifuged at 200xG for 5 minutes at 25°C, and resuspended in 5 mL of complete media. Using a hemacytometer, the number of cells were counted in two 10-µL aliquots to determine the concentration of cells within each suspension. The cells were then diluted to a cell density of 250,000 cells/mL. For each individual well, 0.5 mL of the cell suspension was placed directly on the glass coverslip for 2 hours at which time the wells were filled with 1 mL of fresh media and allowed to culture for 2 days prior to pressure experiments.

Membrane Cholesterol Modifying Treatments

For some experiments, cholesterol/cyclodextran conjugates (CH) were added to the cell preparations, 24 hours after initial seeding. Cells were incubated with 0, 2, 5, 12.5, 25, or 50 µg/mL CH. For each concentration of CH used, 15-mL centrifuge tubes were filled with 7 mL of complete media and the appropriate volume of stock solution (?? µg/mL) of CH (10 µg/mL) was added to achieve the desired concentrations to be used on the cells. The cells were incubated in the desired CH concentrations for an additional 24 hours prior to the start of the pressure experiments or membrane cholesterol quantification procedures (see Membrane Cholesterol Measurements section below).

Pressure System

MC3T3-E1 cell populations (prepared as described above) on glass slides residing in 12-well plates or on gelatin-coated surfaces of tissue culture flasks were exposed to pressure levels above atmospheric using a custom-designed hydrodynamic pressure system (Figure 3) as described previously [62]. This system consisted of a compressed gas tank that delivered pressurized gas mixture (5% carbon dioxide, 95% air gas mixture) to a pressure chamber downstream of a hydrostatic fluid column and humidifying chamber. The desired static pressure was maintained in the pressure chamber by controlling the depth of the tubing in the hydrostatic fluid column. The flow rate of gas from the gas tank (5% carbon dioxide, 95% air gas mixture) and the pressure head on the hydrostatic fluid column were positioned to minimize the amount of gas flow into the pressure chambers while maintaining the experimental pressure regimes and cell viability. The flow rate into the pressure chamber was adjusted using the pressure regulator attached to the 5% carbon dioxide/ 95% air mixture gas tank. The pressure in

the chamber was maintained above the atmospheric pressure in the control chamber using resistive tubing interconnected between them. The outlet of the control chamber was left open to atmosphere to allow gas to vent from the upstream pressure chamber. Thus, the control chamber was maintained at atmospheric pressure, but otherwise, similar experimental gas conditions. Pressures in both chambers were monitored with a Statham blood pressure transducer interfaced to a multi-channel analog to digital converter. The digital output was acquired using Signal Express LabVIEW software on a computer PC, which allowed for continuous, real-time monitoring of the experimental pressures in the chambers to be examined. The pressure and control chambers were maintained at 37°C using a temperature-controlled oven.

For pulsatile pressures, the static pressure set by the hydrostatic fluid column setup served as the mean pressure. Sinusoidal pressures were generated in the pressure chamber with pulse amplitudes ranging from 0 to 20 mmHg at frequencies from 0 to 1 Hz using a bellows pump connected to a linear motor. The linear motor was powered by a DC power supply interfaced to a function generator.

It should be noted that the pulse pressure amplitude achievable by our system depends on the volume of the pressure chamber used to stimulate cells as dictated by the ideal gas law represented in *Equation 1*.

$$P_{max} = \frac{\Delta V}{V_{chamber}} P_{min} \qquad \text{Equation 1}$$

Based on this law, the change in volume (ΔV) needed to oscillate the pressure between the maximum pressure (P_{max}) and the minimum pressure (P_{min}) is governed by

the volume of the chamber, $\boldsymbol{\Delta V}$. $\boldsymbol{\Delta V}$ into our chamber was provided by the stroke volume of our bellows. The limited stroke volume of our bellows is what restricted the achievable pressure amplitudes for our device. By adjusting the chamber volume, we could achieve the desired pulse amplitudes of pressure, albeit at the expense of the number of cells we can test.

To expose cells to the pressure regimes of interest to the present study, we developed custom pressure chamber setups depending on our experimental objectives (shown in Figures 4-6). These chambers were connected downstream of the hydrostatic pressure column shown in the Figure 3. The first pressure chamber setup consisted of using 5-wells of a 12-well plate. One of the wells was designed to be used as a humidifier (shown in Figure 6). Downstream of the humidifying chamber, 4-wells were capped with rubber stoppers to create air-tight seals. These 4-wells were connected in series through ports in the rubber stoppers. By using uniform-sized tubing between wells and resistive tubing serving as the outlet for the last well, each well would be pressurized to the same extent.

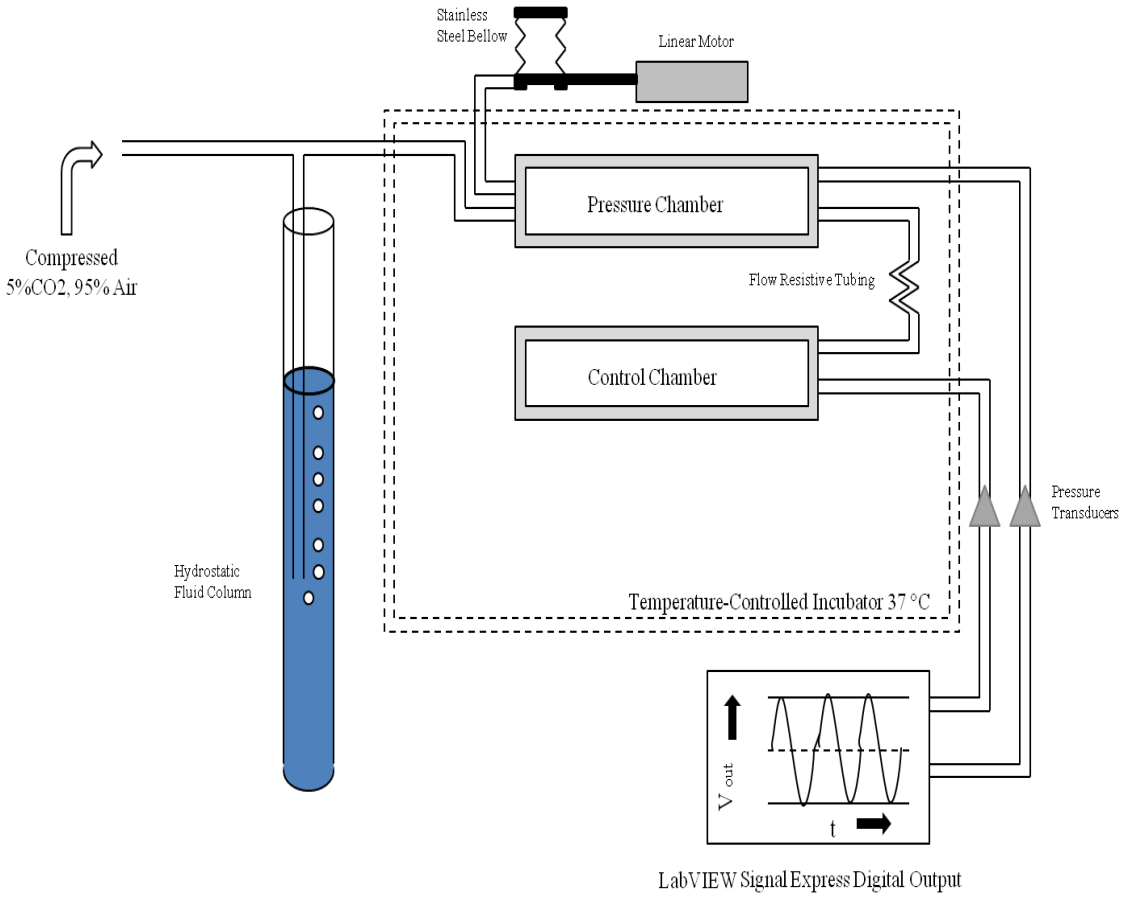

Figure 3: Custom-Designed Pressure System (Adapted via [63]).

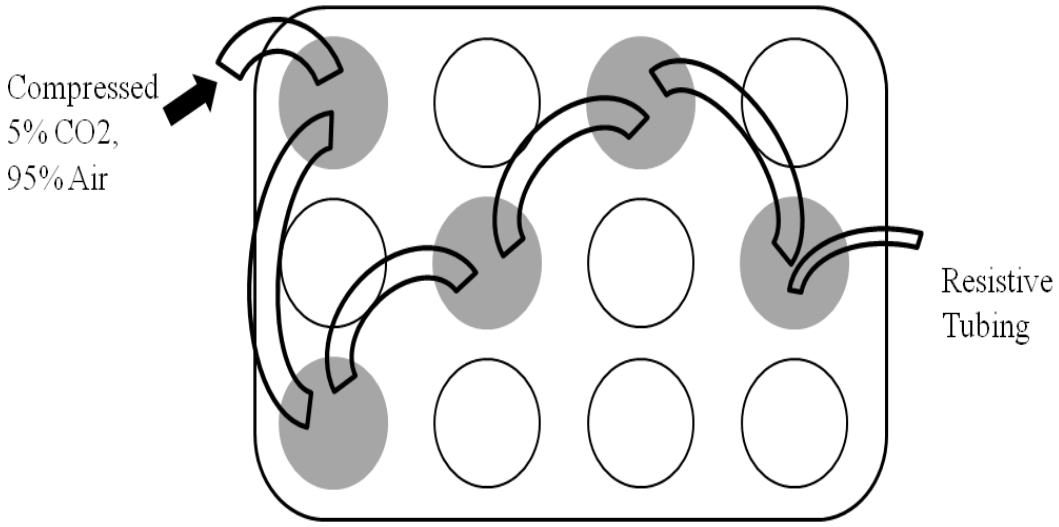

Figure 4: Frontal View of the 12-Well Plate Redesigned Pressure Chamber Used in the Custom-Designed Pressure System Model.

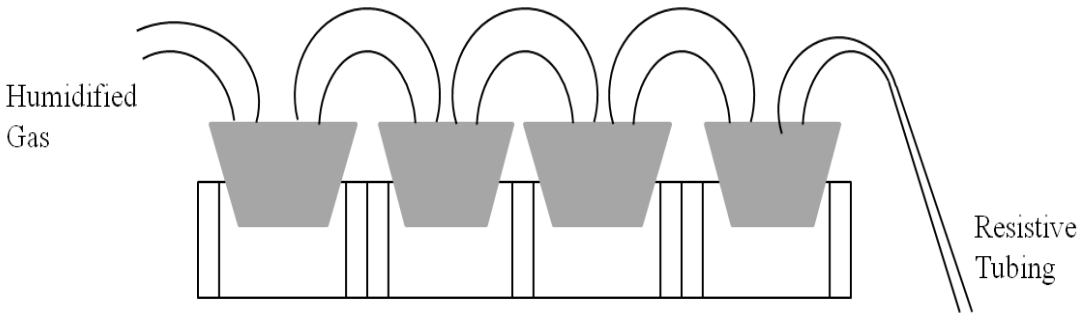

Figure 5: Lateral View of the 12-Well Plate Redesigned Pressure Chamber Used in the Custom-Designed Pressure System Model.

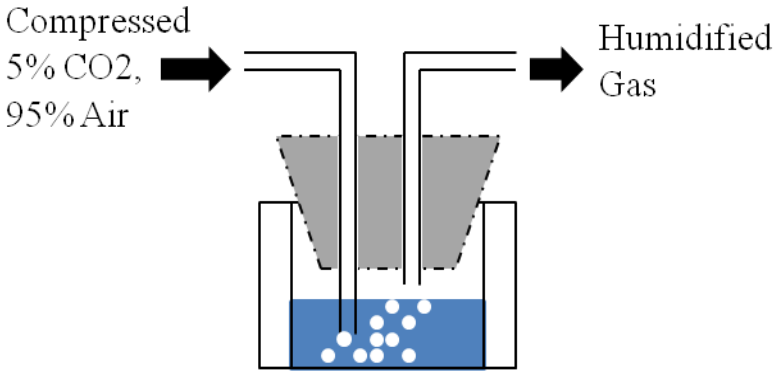

Figure 6: Custom-Designed Humidifier in the 12-Well Plate Used in the Custom-Designed Pressure Chamber.

The second custom-designed chamber was a modified 75 cm^2 tissue culture flask connected downstream of the humidifier of our hydrodynamic pressure system (Figure 7). This setup was used for analyses that required large numbers of cells such as our cell cycle analysis. The flask was sealed with a rubber stopper with two ports. One port served as the inlet for the compressed air mixture to enter the flask chamber. The second port served as the outlet to which resistive tubing was used to connect to a downstream control chamber. A front view of the custom-designed flask chamber is shown in Figure 7. A close-up view of the custom-designed flask chamber is shown in Figure 8.

For experiments, cell preparations were exposed to 40 mmHg static pressure as well as pulsatile pressures with a mean of 40 mmHg and amplitudes of either 10 (i.e., 45/35) or 20 mmHg (i.e., 50/30). Controls for all experiments were cells maintained under atmospheric pressure, but otherwise similar experimental gas, conditions. These pressure regimes were estimated to mimic that which would be generated in bone during single bouts of elevated loading (i.e., impact exercises)[64-68]. Previously, we had shown that there were no differences in the behavior cells maintained in standard incubator conditions and those cultured under atmospheric pressure conditions using our hydrodynamic pressure system [63]. Thus for some experiments, controls were maintained in a standard tissue culture incubator under atmospheric pressures.

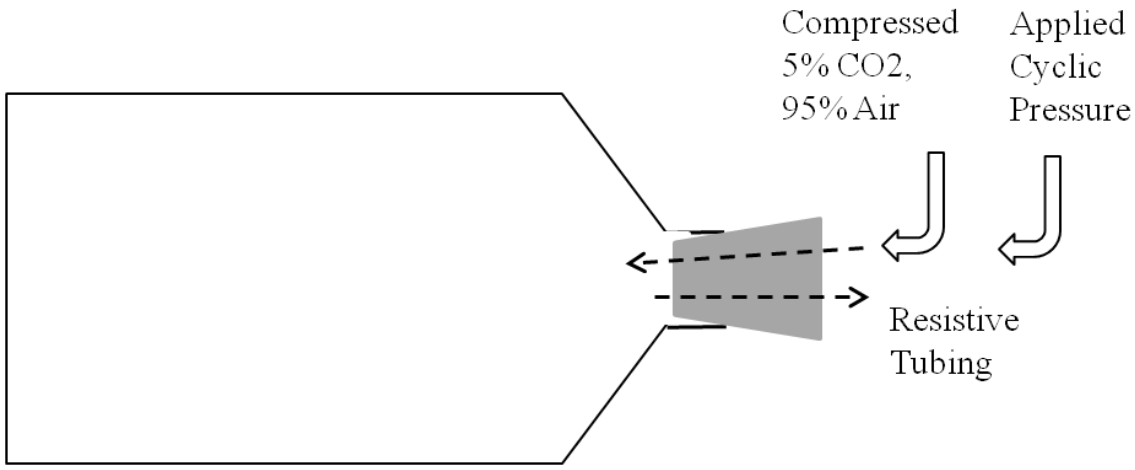

Figure 7: Custom-Designed Pressurized Flask Chamber (Frontal View).

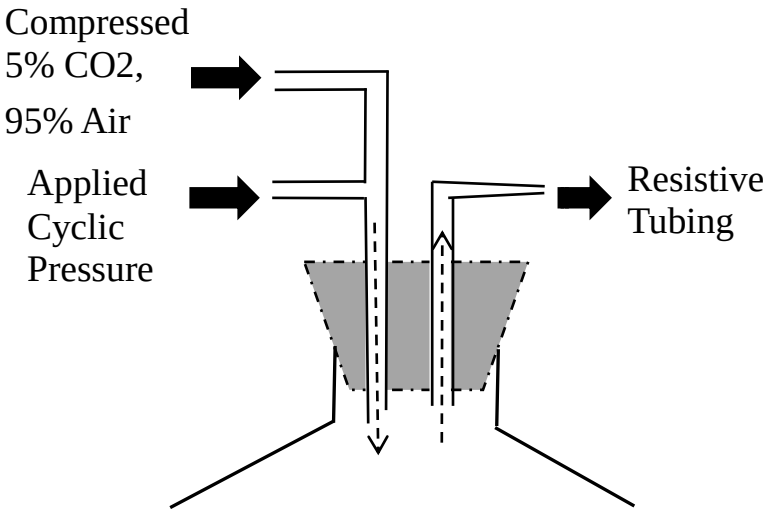

Figure 8: Custom-Designed Pressurized Flask Chamber (Zoomed-In View of Figure 7).

Analysis of Cytoskeletal F-Actin Stress Fiber Formation

Visualization of Cytoskeletal F-actin Stress Fibers

After experiments, the cells were fixed with 4% paraformaldehyde for 20 minutes followed by rinsing three times with PBS for 2 minutes each. The cells were then permeabilized with 0.1% triton X-100 in 1% BSA in PBS for 3 minutes and subsequently washed 3 times with 1% BSA in PBS for 2 minutes each. In preparation for fluorescence staining, the cells were blocked with 1% BSA in PBS for 30 minutes. Next, the cells were fluorescently stained for 1 hour with 7.75 µg/mL Alexa568-red phalloidin (F-actin label) and 1.1667 µg/mL blue-fluorescent DAPI nucleic acid stain. Following three rinses with 1% BSA in PBS for 2 minutes each, the stained cells on coverslips were mounted on glass-slides using Vecta-Shield mounting solution (Vector Laboratories). The coverslips were secured and sealed to the glass slide using nail-polish (i.e., acrylic-based sealant).

Stained cells were visualized using an Olympus (Model IX-70) inverted light microscope interfaced to a high resolution Hammamatsu camera. Images of monolayered cell populations were acquired using 400x magnification in conjunction with brightfield, rhodamine red (excitation/emission wavelength: 570/590 nm), and ultraviolet (excitation/emission wavelength: 358/461 nm) optics. SimplePCI software was used to acquire five random images per well for each treatment group.

To quantify the stress fiber responses of cells, we used ImageJ software to visually analyze our images of fluorescently stained cells. Two main features of the stained cells were analyzed: F-actin stress fiber formation and cell density. F-actin stress fiber positive cells are those within a population with at least one stress fiber running through the center of the cell. For example, in Figure 9, the cell on the left would be

considered stress fiber negative while the cell on the right would be considered stress fiber positive due to the prevalence of linear F-actin stress fibers that navigated through the central region of the cytoplasm. Finally, the cell density was quantified as the number of cells within a microscopic field.

Flow Cytometric Analysis of Cell Cycle

For cell cycle analyses, MC3T3-E1 osteoblastic cells were serum-starved in serum-free MEM Alpha Modification with 1% L-glutamine for 24 hours to synchronize their mitotic activity. At that time, the osteoblast-like cells were exposed to either a 6-hour or 12-hour exposure to a 50/30 mmHg sinusoidal pressure at a frequency of 1 Hz. Controls were parallel cultures maintained at 0 mmHg above atmospheric pressure.

Immediately after experiments, MC3T3-E1 cells were lifted using 0.05 % trypsin, centrifuged at 200xG for 5 minutes at 25°C, and resuspended in 10 mL of ice-cold PBS. The cells were then centrifuged at 200xG for 5 minutes at 25°C and resuspended in 70% ice-cold ethanol overnight. The next day, the cells were washed three times in ice-cold PBS. During these rinses, cells were pelleted by 600xG centrifugation for 8 minutes at 25 °C. After these rinses, the cells were blocked in filtered 1% BSA in PBS to minimize non-specific binding of fluorescent stain and subsequently labeled with 1.1667 µg/mL of DAPI under gentle agitation for 2 hours. Finally, the cells were washed three times with filtered 1% BSA in PBS and resuspended in fresh PBS prior to flow cytometric analyses. An LSR II flow cytometry (Becton-Dickinson) with FacsDIVA (Becton-Dickinson) software was used to analyze cell samples.

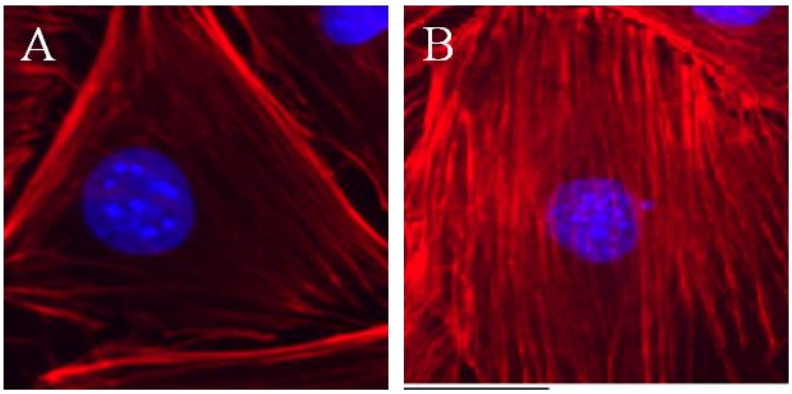

Figure 9: F-actin Stress Fiber Formation of MC3T3 cells. [A] MC3T3 cell with no SFF. [B] MC3T3 cell exhibiting SFF.

Membrane Cholesterol Measurements

Procedures for membrane cholesterol extraction of MC3T3-E1 monolayers were based on the method of Bligh and Dyer [69]. Briefly, MC3T3-E1 cells were lifted using trypsin, centrifuged at 200xG for 5 minutes at 25°C and resuspended in 10 mL of fresh medium. Then the cells were centrifuged at 200xG for 5 minutes at 25°C and resuspended in ice-cold PBS. After vortexing, a 1:3 (v/v) chloroform/methanol solution was added, and the samples were incubated under constant agitation and periodic vortexing for 10 minutes at room temperature. At that time, chloroform and water were added to the mixture for 30 seconds and the entire mixture was centrifuged at 1900xG for 10 minutes at room temperature. The top layer of the supernatant was aspirated off to allow the underlying alcohol layer to be exposed to the atmosphere. The tubes were incubated in a water bath between 40-50°C to evaporate off the remaining layers. After evaporation, the dried cholesterol was reconstituted with 10% triton X-100 in isopropyl-alcohol and stored at -20°C until measurement.

To quantify cholesterol amounts extracted from cells, the reconstituted cholesterol solution was mixed with the color reagent of a Free Cholesterol E kit (Wako) and incubated at 37°C for 5 minutes. A BioTek spectrophotometer was then used to measure the absorbance of these solutions at 600nm (μQuant). The absorbance readings were fitted to a standard curve according to the manufacturer's instructions to determine the concentration of free cholesterol in each sample.

Membrane Fluidity Measurements

Membrane cholesterol was measured based on the methods of Celedon [70]. Briefly, MC3T3-E1 cells were lifted using trypsin, centrifuged at 200xG for 5 minutes at

25°C, and resuspended in pre-warmed PBS. Cells were incubated with 2.5 µM pyrene decanoic acid (PDA; Molecular Probes) in PBS at 37°C under gentle agitation for 1 hour. The cell suspensions were then washed twice with PBS using centrifugation at 600xG for 5 minutes at room temperature. Finally, fluorescence emissions were measured with the cells suspended in PBS. A fluorescence spectrophotometer (Hitachi; F-2500) was used to emit PDA fluorophore at 375 nm and 470 nm wavelengths. The fluorescence emission at 375 nm was used to quantify monomer emissions (I_m), where as the emission at a wavelength at 470 nm represented the excimer emissions (I_e) under 344 nm excitation [30].The ratio of monomer/excimer emissions (Ie/Im) was used as a quantitative measure of membrane fluidity.

Statistical Analysis

Data was expressed as mean ± standard error. The experimental treatment means were compared using a Student's t-test with Bonferroni adjustment with $p < 0.05$ indicating a significant difference. Sigma Plot software was used to conduct Pearson's Correlation Coefficient (r) analysis to measure the strength of association between two variables with positive (+) and negative (-) correlations.

Results

Generating Hydrostatic & Cyclic Pressures

LabVIEW Signal Express software interfaced to a pressure transducer was used to monitor the hydrostatic or cyclic pressures generated in the pressure chambers. Figure 10 shows representative computer outputs used to ensure the osteoblastic cells were exposed to the pressure of interest to the present study. These include a static 40 mmHg pressure level and two different 1-Hz sinusoidal pressure regimes with a mean of 40 mmHg and amplitudes of either 10 or 20 mmHg.

Pressurize-Sensitive Stress Fiber Formation

SFF by MC3T3 osteoblast-like cells exposed to the pressure regimes tested in the present study are displayed visually (Figure 11). As shown in Figure 11, cells that had been maintained under control pressure conditions (CTL) displayed the least amount of SFF formation in comparison to those exposed to either 40 mmHg static pressure as well as either 45/35 or 50/30 mmHg cyclic pressures at 1 Hz for 2 hours.

Quantitatively, MC3T3 cells exposed to all pressure conditions exhibited significantly ($p < 0.05$) enhanced SFF compared to control cells (Figure 12). According to Figure 12, cyclic pressure with a mean of 40 mmHg and amplitude of 20 mmHg at a frequency of 1 Hz showed the greatest amount of SFF compared to all exposed pressure conditions. In this regard, the amount of stress fiber formation by the cells depended on the amplitude of pressure with cyclic pressures inducing the greatest amount of SFF by MC3T3-E1 osteoblastic cells (Figure 11 & 12).

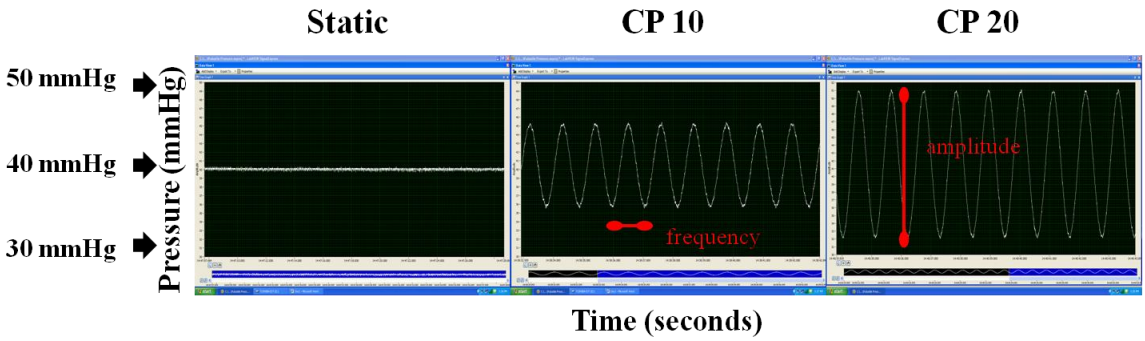

Figure 10: LabVIEW Signal Express Sinusoidal Waveforms of Static (SP) and Cyclic Pressures (CP 10 & CP 20). Static pressure (SP) was held at 40mmHg, (CP 10) cyclic pressure with a mean pressure of 40mmHg and amplitude of 10mmHg at a frequency of 1 Hz, and (CP 20) Cyclic Pressure with a mean pressure of 40mmHg and amplitude of 20mmHg at a frequency of 1 Hz.

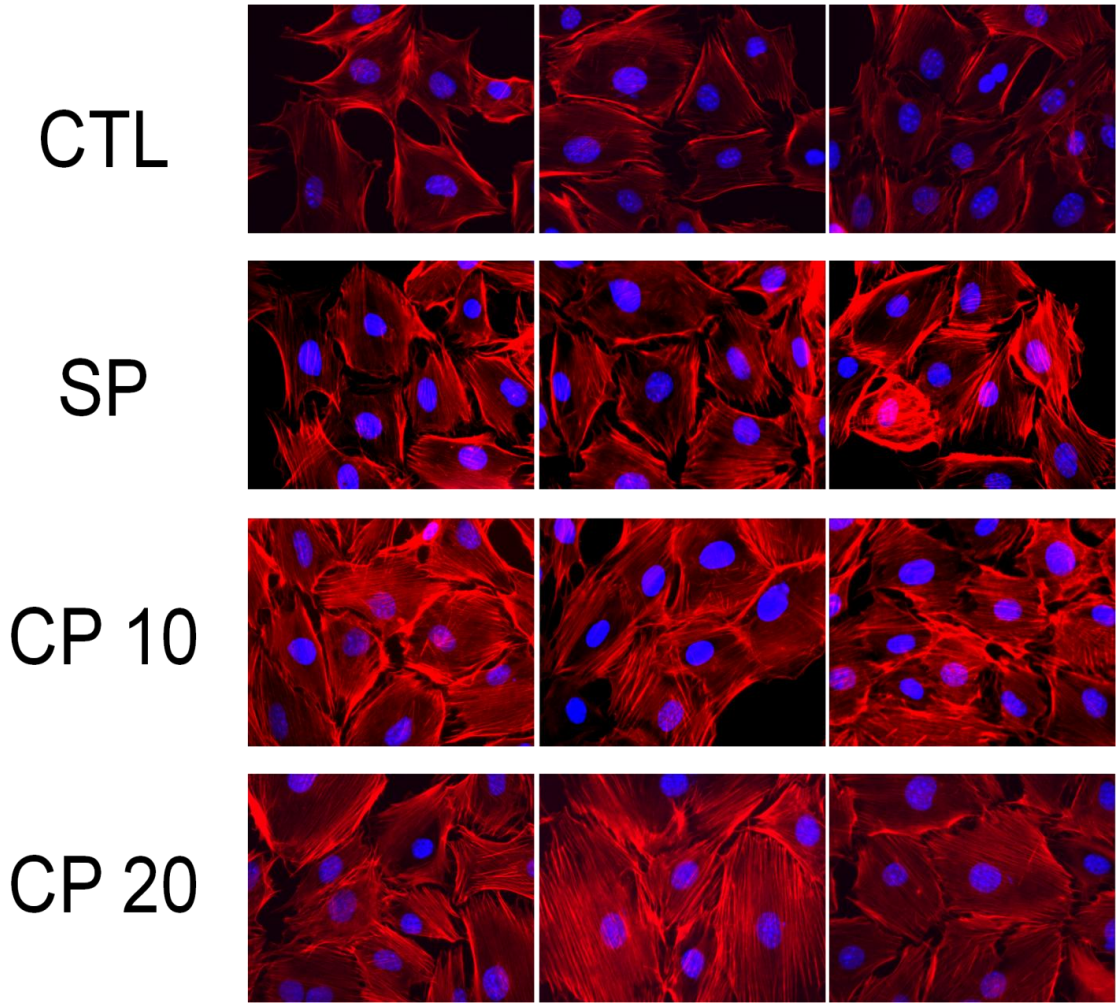

Figure 11: Stress Fiber Formation by MC3T3-E1 Cells is Dependent on the Amplitude of the Applied Pressure Regime. Three representative images of cells that had been fluorescently stained using phalloidin (actin stain; red) and DAPI (nuclear stain; blue) after exposure to 0 mmHg (CTL), 40 mmHg (SP), 45/35 mmHg (CP 10) or 50/30 (CP 20) at a frequency of 1 Hz for 1 hour. Images were taken at 400X magnification.

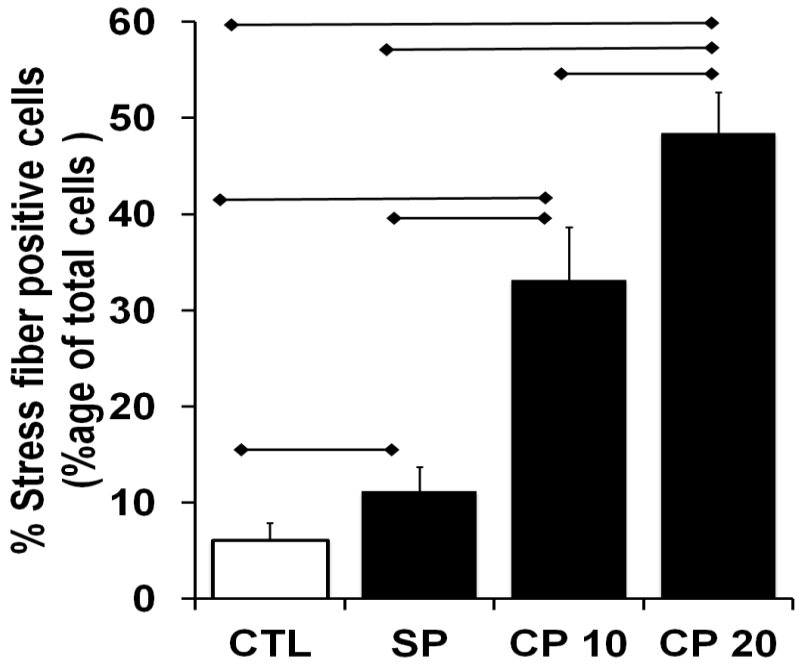

Figure 12: Stress Fiber Formation by MC3T3-E1 Cells is Dependent on the Amplitude of the Applied Pressure Regime. Pressure conditions shown are control (CTL) of 0 mmHg, static pressure (SP) of 40 mmHg, cyclic pressure (CP 10) with a mean of 40 mmHg and amplitude of 10 mmHg, and cyclic pressure (CP 20) with a mean of 40 mmHg and amplitude of 20 mmHg. All vertical bars in are mean values ± SEM with horizontal lines depicting $p<0.05$ using paired Student's t-test with Bonferroni's multiple comparisons tests (n=8).

Effects of Pressure on Cell Density

The average MC3T3 cells per field used in analyzing the stress fiber formation data were recorded. As indicated in Figure 13, the cell density levels of all pressure conditions were similar to those of controls. Therefore, changes in SFF occurred without any changes in cell density.

Effects of Pressure Stimulation on the Mitotic Activity of MC3T3-E1 Osteoblastic Cells

In order to determine if pressure plays a role in the mitotic activity of osteoblast-like cells, a cell cycle analysis was conducted for MC3T3-E1 cells exposed to 40 mmHg static pressure for 6 (Figure 14 & Table 1) and 12 (Figure 16 & Table 2) hours. Compared to controls, the numbers of cells in the S-phase after exposure to 40 mmHg for 6 hours were significantly ($p<0.05$) elevated relative to non-pressurized cells (Figures 14 & Table 1).

After 12 hours, the numbers of pressurized cells in the G2m, but not in the G1 and S, phases was significantly ($p<0.05$) elevated (Figure 15 & Table 2). Combined, these data suggested that exposure to 40 mmHg pressure has a transient effect on osteoblastic cell mitotic activity.

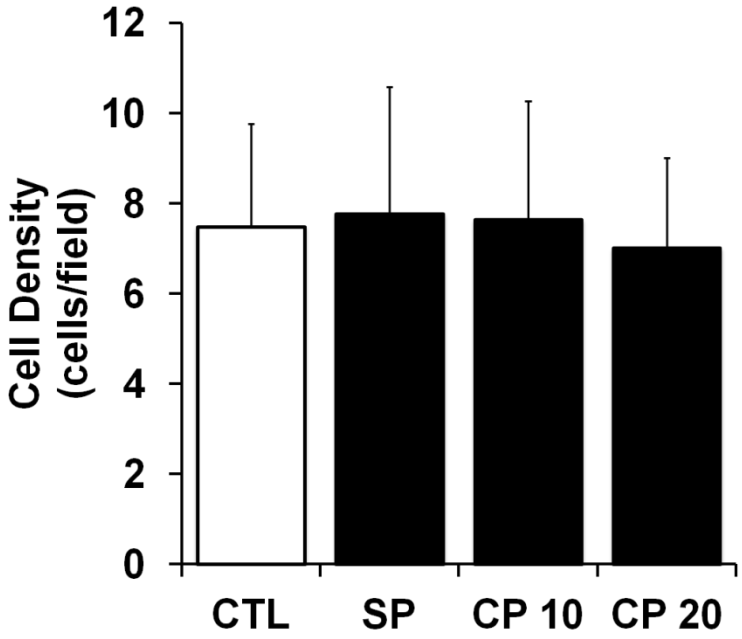

Figure 13: Stress Fiber Formation by MC3T3-E1 Cells is Independent of Cell Density. The pressure conditions shown are control (CTL) of 0 mmHg, static pressure (SP) of 40 mmHg, cyclic pressure (CP 10) with a mean of 40 mmHg and amplitude of 10 mmHg, and cyclic pressure (CP 20) with a mean of 40 mmHg and amplitude of 20 mmHg. All vertical bars are mean ± SEM with horizontal lines depicting $p<0.05$ using paired Student's t-test; n=8.

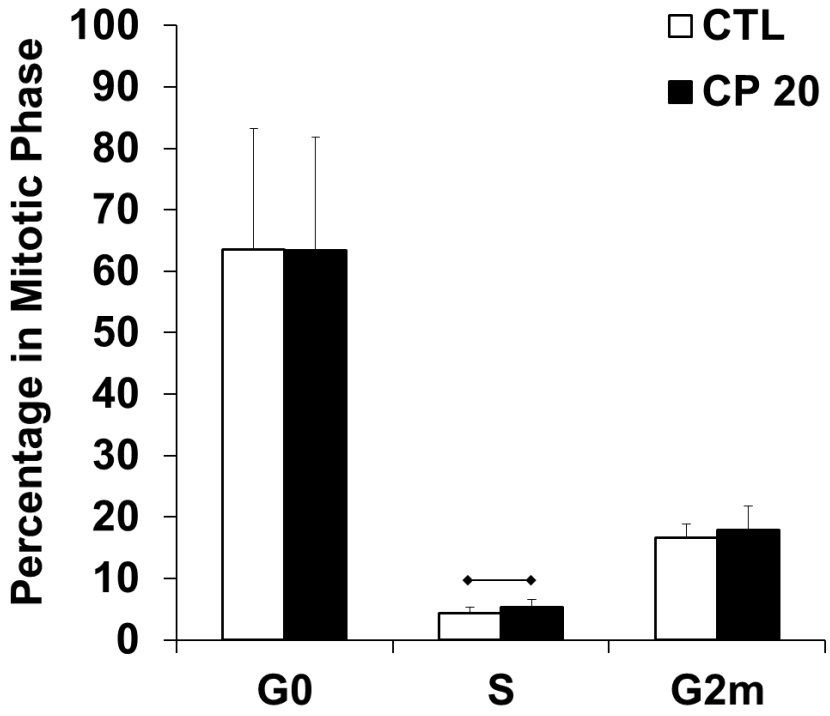

Figure 14: Pressure Exposure Alters the Mitotic Activity of MC3T3 Cells in the S-Phase After 6 hours. The percentage of MC3T3 cells during each mitotic phase exposed to either 0 mmHg (CTL) or 50/30 mmHg (CP 20) at a frequency of 1 Hz for 6 hours. All vertical bars are mean values ± SEM with horizontal lines depicting $p<0.05$ using paired Student's t-test; n=4.

Table 1: Pressure Exposure Alters the Mitotic Activity of MC3T3 Cells in the S-Phase After 6 hours. The average percentage plus or minus the standard deviation of MC3T3 cells during each mitotic phase after exposure to either 0 mmHg (CTL) or 50/30 mmHg (CP 20) at a frequency of 1 Hz for 6 hours. Values are mean ± SEM

	CTL	CP 20
G0	63.6 ± 19.74	63.4 ± 18.40
S	4.3 ± 0.93	5.4 ± 1.18
G2m	16.7 ± 2.21	17.9 ± 3.85

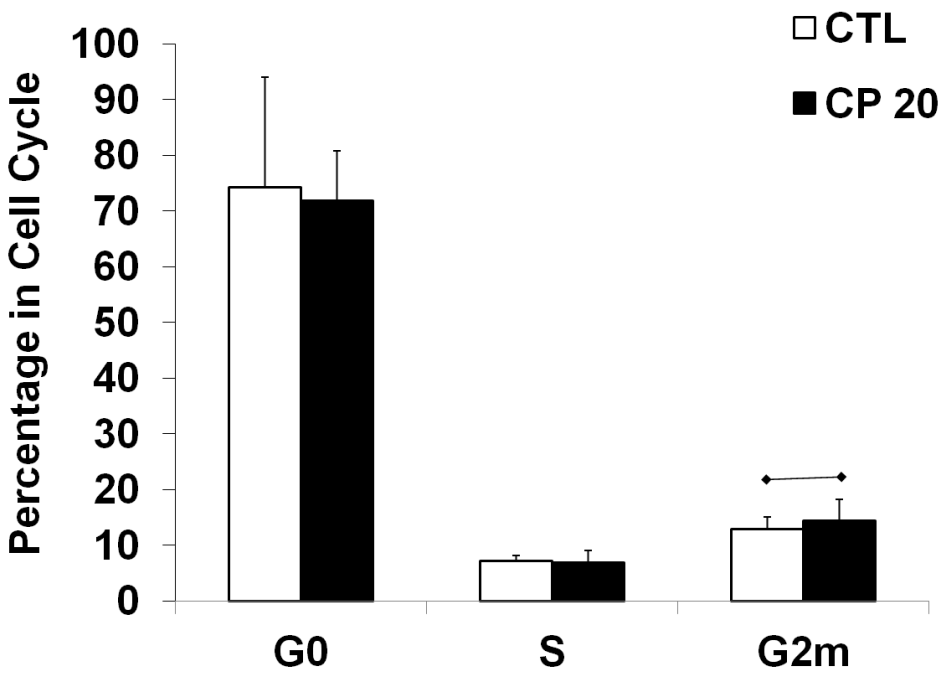

Figure 15: Pressure Exposure Alters the Mitotic Activity of MC3T3 Cells in the G2m-Phase After 12 hours. The percentage of MC3T3 cells during each mitotic phase after exposure to either 0 mmHg (CTL) or 50/30 mmHg (CP 20) at a frequency of 1 Hz for 12 hours. All vertical bars are mean values ± SEM with horizontal lines depicting $p<0.05$ using paired Student's t-test; n=4.

Table 2: Pressure Exposure Alters the Mitotic Activity of MC3T3 Cells in the G2m-Phase After 12 hours. The average percentage plus or minus the standard deviation of MC3T3 cells during each mitotic phase exposed to either 0 mmHg (CTL) or 50/30 mmHg (CP 20) at a frequency of 1 Hz for 12 hours. Values are mean ± SEM.

	CTL	CP 20
G0	74.3 ± 6.74	71.9 ± 8.81
S	7.2 ± 2.13	6.9 ± 2.25
G2m	12.9 ± 4.15	14.4 ± 3.80

Effects of *Exogenous Cholesterol*

Effects of Exogenous Cholesterol on Stress Fiber Formation

Stress fiber formation exhibited by MC3T3-E1 cells pretreated with 0 - 50 μg/mL cholesterol-cyclodextrin conjugates and subsequently maintained under control (0 mmHg) conditions or exposed to different pressure regimes (mean of 40 mmHg with amplitudes between 0-20 mmHg, frequency 1 Hz) is shown visually (Figure 16) and quantitatively (Figure 17). Control cells (Figure 16, CTL) visibly have the least amount of SFF than pressurized cells (Figure 17, SP and CP20). Moreover, cells exposed to either static or cyclic pressure appeared to have the highest numbers of SFF cells.

MC3T3 cells pretreated with 0 – 12.5 μg/mL cholesterol-cyclodextrin conjugates prior to cyclic pressure (CP20) exposure exhibited significantly ($p<0.05$) more SFF than control (CTL) cells (Figure 17). The amount of SFF by the cells pretreated with 0 – 12.5 μg/mL cholesterol-cyclodextrin depended on the amplitude of pressure. In contrast, at cholesterol-cyclodextrin conjugates from 25 and 50 μg/mL, MC3T3 SFF did not depend on the amplitude of the applied pressure (Figure 17).

Effects of Exogenous Cholesterol and Pressure on Cell Density

According to Figure 18, cholesterol-cyclodextrin conjugates have no effect on cell density. As a result, changes in stress fiber formation for all membrane cholesterol concentrations occurred without any changes in cell density.

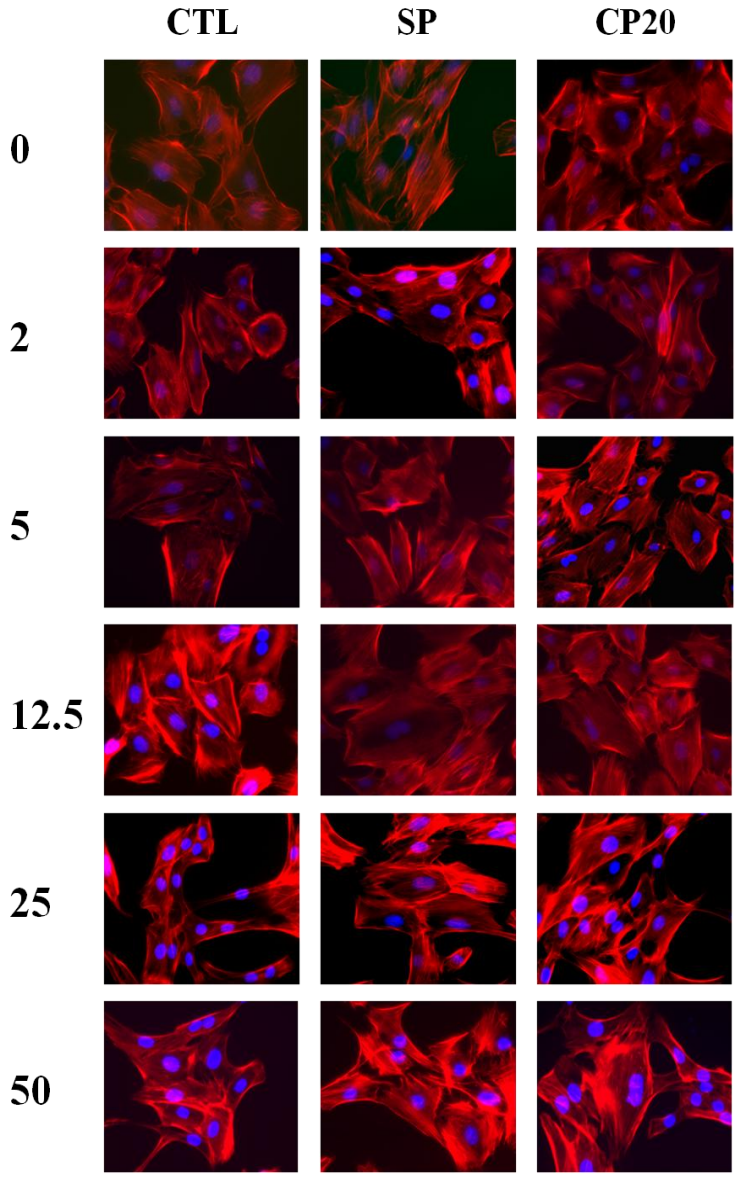

Figure 16: Exogenous Cholesterol Enrichment Alters the Stress Fiber Formation Responses of MC3T3 Osteoblast-like Cells. MC3T3 cells depicting the effects of 0, 2, 5, 12.5, 25, and 50 µg/mL cholesterol/cyclodextran conjugates on pressure-sensitive stress fiber formation (n=8) exhibited by MC3T3-E1 cells exposed to either 0 mmHg (CTL), 40mmHg (SP), or 50/30 mmHg (CP20) at a frequency of 1 Hz for 1 hour. The cells were fluorescently stained using phalloidin (actin stain; red) and DAPI (nuclear stain; blue) to exhibit stress fiber formation. Images were taken at 400X magnification.

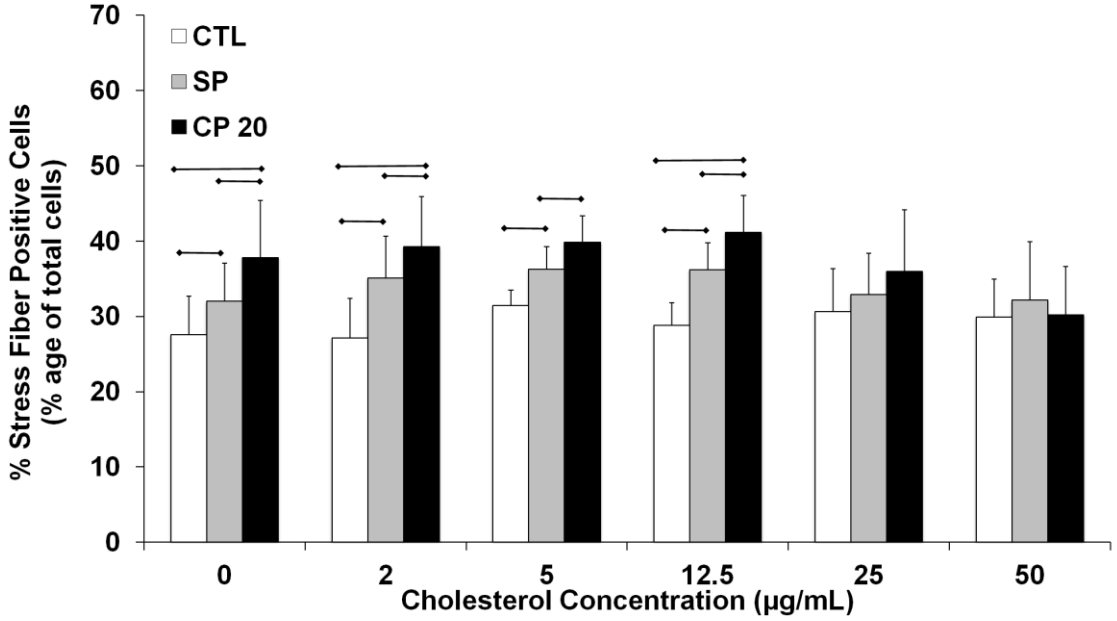

Figure 17: Exogenous Cholesterol Enrichment Alters the Stress Fiber Formation Responses of MC3T3 Osteoblast-like Cells. MC3T3 cells depicting the effects of 0, 2, 5, 12.5, 25, and 50 µg/mL cholesterol/cyclodextran conjugates on pressure-sensitive stress fiber formation exhibited by MC3T3-E1 cells exposed to either 0 mmHg (CTL), 40mmHg (SP), or 50/30 mmHg (CP20) at a frequency of 1 Hz for 1 hour. Vertical bars are mean ± SEM. Horizontal lines indicate significant ($p<0.05$) differences using Student's t-test with Bonferroni's multiple comparison tests; n=8.

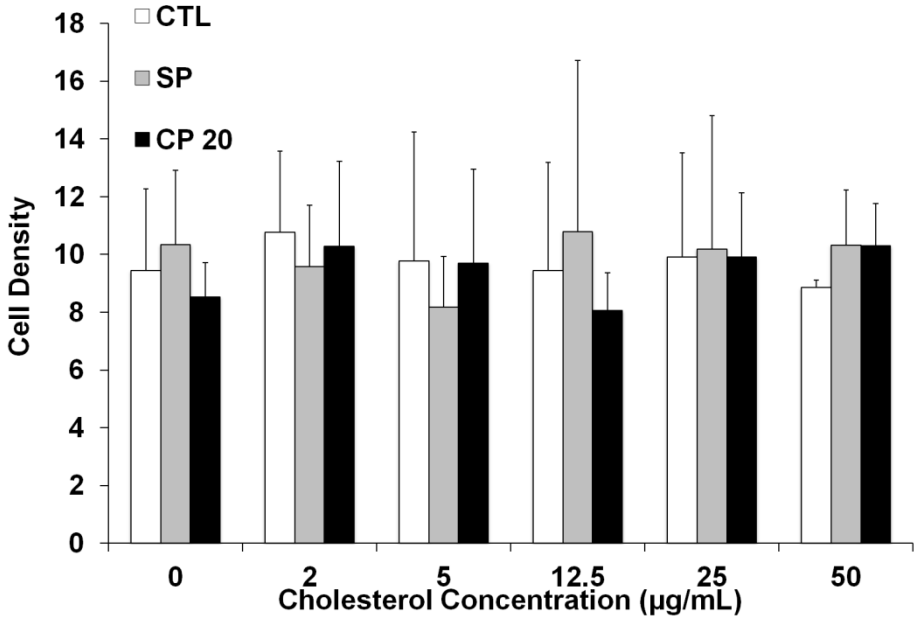

Figure 18: Exogenous Cholesterol Enrichment Alters the Stress Fiber Formation Responses of MC3T3 Osteoblast-like Cells Independent of Cell Density. MC3T3 cells depicting the effects of 0, 2, 5, 12.5, 25, and 50 µg/mL cholesterol/cyclodextran conjugates on the cell density levels exhibited by MC3T3-E1 cells exposed to either 0 mmHg (CTL), 40mmHg (SP), or 50/30 mmHg (CP20) at a frequency of 1 Hz for 1 hour. Bars are mean ± SEM; n=8.

Effects of Exogenous Cholesterol on the Membrane Fluidity and Membrane Cholesterol of MC3T3 Cells

Membrane cholesterol participates in the cellular signaling through its impact on membrane fluidity. According to Figure 19, MC3T3 cells treated with increasing concentrations of extracellular cholesterol complexes (between 0 to 50 µg/mL) resulted in gradual increases in membrane cholesterol levels. According to Figure 20, the average membrane fluidity gradually decreased as a function of cholesterol-cyclodextrin conjugate concentration up to 12.5 µg/mL. Beyond this concentration and up to 50 µg/mL cholesterol-cyclodextrin conjugation, membrane fluidity appeared to have plateaued. Based on this data, extracellular cholesterol concentrations altered the membrane cholesterol levels in MC3T3 cells (Figure 19) with a possible impact on membrane fluidity (Figure 20).

According to our previous data, exogenous cholesterol conjugates alter the membrane cholesterol of MC3T3 cells (Figure 19) and altered membrane fluidity (Figure 20). A correlation analysis was conducted to test inter-dependence between exogenous cholesterol concentrations, membrane cholesterol, and membrane fluidity shown in Table 3. The concentration of cholesterol conjugates used to treat cells positively correlated ($r = 0.902$, $p = 0.0139$) with membrane cholesterol amounts (Table 3). In addition, the membrane cholesterol amounts negatively correlated ($r = -0.896$, $p = 0.0156$) with membrane fluidity (Table 3). These results indicate evidence that the amount of cholesterol cyclodextran conjugate altered the membrane fluidity via an impact on membrane cholesterol abundance within MC3T3 cells.

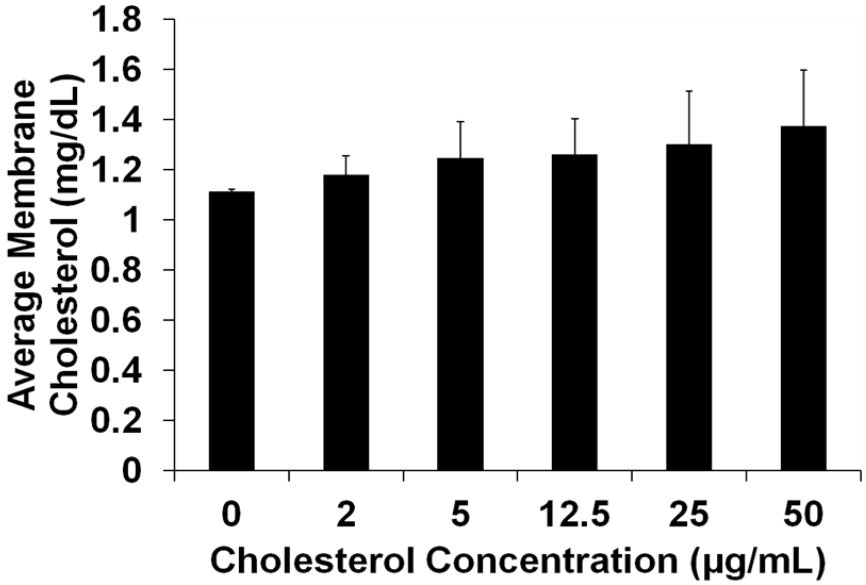

Figure 19: Exogenous Cholesterol Enrichment Alters the Average Membrane Cholesterol of MC3T3 Osteoblast-like Cells. Depicts the effects of 0, 2, 5, 12.5, 25, and 50 µg/mL cholesterol/cyclodextran conjugates on the averaged membrane cholesterol of MC3T3 cells. Vertical bars are mean ± SEM; n=3.

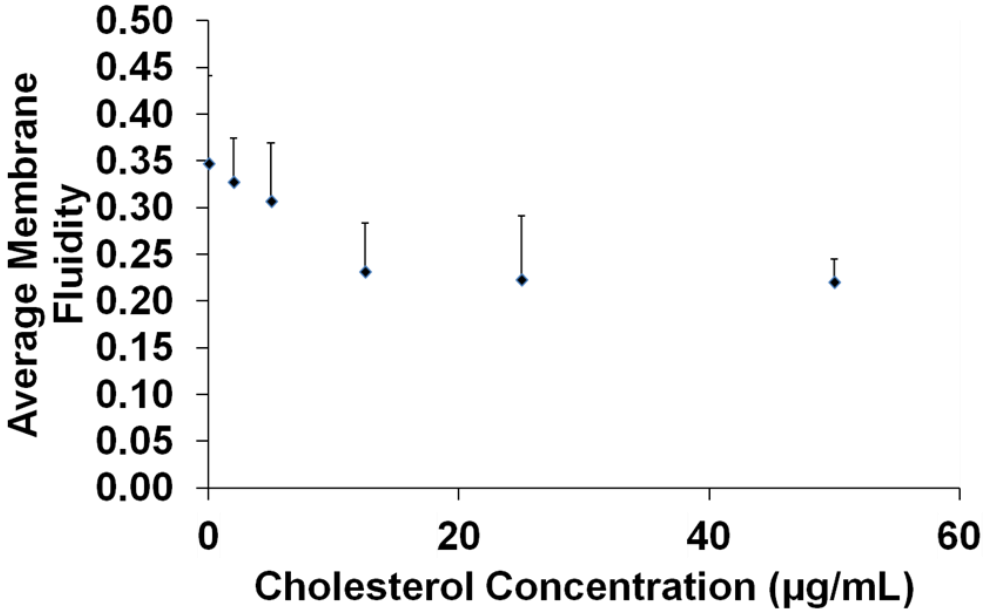

Figure 20: Exogenous Cholesterol Enrichment Alters the Average Membrane Fluidity of MC3T3 Osteoblast-like Cells. Depicts the effects of 0, 2, 5, 12.5, 25, and 50 µg/mL cholesterol/cyclodextran conjugates on the averaged membrane fluidity of MC3T3 cells. The vertical lines above the data points indicates one standard deviation from the average membrane fluidity; n=8.

Table 3: Exogenous Cholesterol Enrichment Alters the Membrane Cholesterol and Membrane Fluidity Responses of MC3T3 Osteoblast-like Cells. A correlation analysis depicting a Pearson r-value coefficient (top number) and a two-tailed p-value (bottom number).

		Cholesterol Amount	Membrane Cholesterol	Membrane Fluidity
Cholesterol Amount	Pearson r p (two-tailed)	-	-	-
Membrane Cholesterol	Pearson r p (two-tailed)	0.902 0.0139	-	-
Membrane Fluidity	Pearson r p (two-tailed)	-0.802 0.0552	-0.896 0.0156	-

Discussion

This study explored the possibility that extracellular cholesterol levels influence the osteoblast mechanosensitivity to fluid pressure via an impact on the cell membrane. Osteoblasts are mechanoreceptive cells that respond to forces such as compression, strain, and shear stress [71]. During normal bone remodeling, osteoblasts have been shown to be mechanosensitive to stresses typical of those generated in the bone matrix environment due to mechanical loading at the tissue level. Mechanical stimuli, such as hydrodynamic pressure, has been shown to stimulate SFF in MC3T3-E1 cells indicating a pressure response [38]. The present study also showed that static and cyclic pressures promote SFF formation relative to cells under control (atmospheric) pressure conditions.

To model cholesterol elevations in the bone matrix environment in the in vitro setting, exogenous cholesterol, in the form of cholesterol-loaded cyclodextrin, was added to MC3T3-E1 cultures at various concentrations up to 50 µg/mL. These studies supported the possibility that a cholesterol overabundance in the bone cell environment is capable of altering the responsiveness of osteoblastic cells to pressure stimulation possibly through an effect on the cell membrane chemistry.

Hydrostatic & Cyclic Pressure Responsiveness of Osteoblasts

There is an accumulation of data supporting the likelihood that mechanical loading on bone due to daily physical activities, such as walking, running, and exercising, stimulates bone cells in the mineralized matrix and, in doing so, plays an important role in bone health [26, 72, 73]. Conceivably, as the ability of osteoblasts to sense forces is altered, a progression of bone disease may develop, such as osteoporosis. Previous

studies have shown that osteoblastic cells (e.g., osteocytes) serve as mechanosensor cells for bone [46]. By monitoring the formation of f-actin stress fibers by osteoblastic cells in response to a pressure, the present study assessed their mechanosensitivity to this stimulus. In this regard, the focus of this study was to provide insight into how MC3T3-E1 osteoblastic cells respond to dynamic pressure loading and how membrane cholesterol enrichment affects their responsiveness.

Notably, the osteoblastic cells tested in this study exhibited a higher sensitivity to cyclic pressures in comparison to an equivalent static pressure level. Notably, the cyclic pressures (30-50 mmHg) and frequencies (1 Hz) used in this study were in the range predicted to occur in the bone matrix, i.e. 8.6 kPa (65 mmHg) [74] and up to 3 MPa (22,500 mmHg) [48, 51]. Previous theoretical models estimated that fluid pressures in Haversian canals, where osteoblastic cells may reside, would be around 19% of the applied stress with the local pressures reaching a maximum of over 3.4 MPa (25,500 mmHg) or a 18 MPa (135,000 mmHg) in cortical bone [75]. Previous in vitro studies exposed osteoblasts to peak hydraulic pressures varying between 8.6 kPa (65 mmHg) to 3 MPa (22,500 mmHg) [54, 74] compared to our study using a pressure regime of 30 to 50 mmHg (4 to 7 kPa). The approximate stride frequency for human walking is around 0.7-1.2 Hz, therefore this study used a frequency of 1 Hz [76]. In response to mechanical loadings, actin monomers polymerize into stress fibers in bone cells [34]. Stress fiber formation, by osteoblast-like cells has been shown to be a robust marker of their mechanoresponsiveness to mechanical loading [77].

Cytoskeleton Response

Previous studies have shown that MC3T3 cells exhibit f-actin SFF in response to cyclic pressures as high as 5MPa (37,500 mmHg) at a frequency of 1Hz [78]. F-actin SFF is one of the typical responses of cells to mechanical stresses [79] including pressures. We therefore used F-actin stress fiber formation as a way to measure the pressure sensitivity of cells. The highest degree of SFF was seen for osteoblastic cells exposed to cyclic pressures (Figure 12). Therefore, MC3T3 cells appear to be mechanosensitive to pressure, showing the strongest sensitivity to dynamic loadings.

Cell Cycle Analysis

Previous research has indicated that the cell cytoskeleton plays a role in cell mitosis [80]. In order to determine if pressure sensitive changes in osteoblast activity manifests as a functional response, a cell cycle analysis was conducted for MC3T3 cells exposed to 6- and 12- hour pressure to assess its effects on cell proliferation/mitotic activity. Based on our results (Figures 14 & 15), exposure to pressure appears to promote a transient up-regulation of MC3T3 cell passage through the cell cycle that lasts between 6 and 12 hours. This transient increase in cell cycle progression in MC3T3-E1 cells is similar to how a mechanical stimulus stimulates cell cycle progression of other cells, e.g. cancer cells [81]. The transient increase in proliferation of MC3T3-E1 cells supports the possibility that pressure induces a mitotic effect. Previous studies have shown that hypercholesterolemia is linked to decreased proliferation rates in bone cells [16]. Enhanced cholesterol in the microenvironment of osteoblasts may affect their proliferative capacity by influencing the mechanoregulation of the osteoblasts.

Cholesterol-Related Stress Fiber Formation Response of Osteoblasts to Pressure

Cholesterol is an important regulator of cellular membrane fluidity [82]. This study addresses the possibility that the changes in the membrane fluidity due to elevations in extracellular cholesterol alters the ability of the bone cells to sense a pressure change. One way that mechanotransduction plays a role in osteoblast function is proposed to involve structural shifts in the mechanosensors that are embedded in the cell membrane [83]. The deformation behavior and flexibility of the mechanosensors may depend upon the fluidity of the cell membrane. Since cholesterol regulates this fluidity, it is possible that changes in membrane cholesterol content can alter the ability of bone cells to sense pressure changes.

Exogenous cholesterol appears to dose-dependently alter the osteoblast stress fiber responses to the pressure stimuli used in this study. For each cholesterol-cyclodextrin conjugate concentration, MC3T3 cells under control pressures (0 mmHg) displayed the least amount of SFF compared to cells exposed to static (40 mmHg) or cyclic pressures (50/30 mmHg), except at a cholesterol conjugate concentrations of 25 and 50 µg/mL (Figures 16 & 17). Exogenous cholesterol thus appears to play a role in altering the bone cell SFF response to pressure.

Membrane Cholesterol & Fluidity Response

Cholesterol plays a major role in the interaction between the bone cell membrane and the bone cell stress fiber formation [84]. In addition, cholesterol has been shown to affect membrane fluidity and cell proliferation [85]. According to this study, the amount of membrane fluidity decreases as the amount of membrane cholesterol increases until it reaches a plateau between 12.5 to 50 μg/mL of cholesterol (Figures 19 & 20). Since the membrane fluidity of the cell changes the signaling pathway on the cell membrane, this plateau result may explain the membrane cholesterol blockade of the SFF responses of MC3T3-E1 cells to pressure that occurred when the cells were treated with extracellular cholesterol at concentrations between 25 to 50 μg/mL. As expected, there is a significant correlation between the membrane cholesterol and amount of cholesterol conjugate added to the MC3T3-E1 cells (Table 3). Also, there is a significant correlation ($p < 0.05$) between membrane cholesterol and membrane fluidity (Table 3). Thus, the attenuating effects of exogenous cholesterol on the MC3T3-E1 osteoblast cell response to pressure may involve changes in membrane fluidity.

Taken together, the results of the present study implicate membrane cholesterol levels as a determinant of the mechanosensitivity of osteoblasts to pressure via its effect on the cell membrane.

Conclusions

In summary, the present study provided evidence that extracellular cholesterol elevations influence the mechanosensitivity of MC3T3-E1 cells to pressure stimuli . The degree of SFF formation was dependent upon the amplitude of the applied cyclic pressure. The results of the present study also suggest that the osteoblast sensitivity to pressure is subject to modification by extracellular cholesterol levels potentially via an impact on the cholesterol abundance in the cell membrane. These results lay a foundation for an explanation related to the negative impacts of hypercholesterolemia on osteoporosis for future collaborative research efforts to develop novel diagnostic, clinical, and/or dietary strategies

Future Directions

While we provided indirect evidence that cholesterol modification of the cell membrane and its impact on membrane fluidity alters osteoblast sensitivity to pressure, future studies should be conducted to provide more direct evidence. This includes the possibility of using biochemical approaches such as membrane fluidizers (benzyl alcohol) to counteract the membrane rigifying actions of cholesterol and its impact on osteoblast pressure responses (e.g., SFF). In addition, it has yet to be determined whether the effects of membrane cholesterol on osteoblast SFF in response to pressure translates to a detrimental effect on pressure-sensitive regulation of MC3T3-E1 cell proliferation. Finally, it is necessary to translate this data from an in vitro study into an in vivo environment. This can be accomplished using hypercholesterolemic animal models to support the possibility that dysregulated osteoblast mechanotransduction may explain the link between hypercholesterolemia and osteoporosis.

Appendix

Background and Rationale

Recent studies [86] showed that hypercholesterolemia is associated with the onset/progression of osteoporosis but the underlying mechanism is unknown. Osteoporosis develops from dysregulated bone remodeling involving an imbalance between the rate of bone formation by osteoblasts, the bone forming cells, and the activity levels of osteoclasts, the bone resorbing cells. Bone cells of the osteoblastic lineage (particularly the osteocytes) have been shown to be responsible for directing the bone remodeling process. Since a large population of osteoblastic cells reside in the bone matrix in close proximity to the highly vascularized marrow spaces and cortical bone blood supply in the Haversian canal, cholesterol in the blood may conceivably diffuse into the microenvironment of the osteoblasts where it is taken up by their cell membranes [87]. In this pilot study, we set out to determine whether we could use a murine model of hypercholesterolemia for future in vivo investigations regarding a potential relationship between hypercholesterolemia, impaired bone remodeling, and impaired pressure sensitive regulation of osteoblast activity.

For this study, we used femurs collected from lipoprotein receptor-deficient (LDLR-/-) that had been fed either a high fat (HFD) or normal (ND) diet. The bones used in this pilot study were harvested from mice that had been used for a prior study [30]. These mice exhibited elevated blood cholesterol levels after 2, 4, and 8 weeks compared to normal diet types [30]. The main objective of this study was to show that the time-

dependent onset and progression of hypercholesterolemia in the circulation due to high fat dieting for up to 8 weeks is sufficient to enhance free cholesterol levels in bone.

Methods

Mice Cholesterol Quantification

Femurs were extracted from anesthetized LDLR-/- mice that had been stored at -80^{o}C after being subjected to non-invasive blood flow measurements and subsequently euthanized by thoracotomy and exsanguinations for another study [30]. Prior to euthanasia, the LDLr-deficient mice (LDLr-/-) (male; 7-week; Jackson Laboratories; Cat. # 2207) had been fed either normal mice chow diet (ND) or a saturated fat diet (HFD) (21% wt/wt fat and 0.15% wt/wt cholesterol; Harlan Teklad; Cat. # TD88137) for 2, 4, and 8 weeks to induce hypercholesterolemia, which was confirmed as reported [30]. As a basis of comparison, an equivalent number of age-matched LDLR-/- mice were fed ND. Femurs from these mice served as our normocholesterolemic controls. After being euthanatized, mice were weighed (values reported previously[30]) and the femurs from the right and left hind limbs were dissected out and immediately frozen, as is, at -80^{o}C.

During a previously described investigation using the same mice from which femurs were collected, blood (approximately 500 µL) had been harvested by thoracotomy followed by cardiac puncture. As part of these earlier studies, plasma levels of total and free blood cholesterol levels were measured and shown to be affected by diet type (HFD vs. ND) and duration (2, 4, or 8 weeks), as expected[30]. Table 4 summarizes the blood cholesterol concentrations of the LDLr-deficient mice subjected to ND or HFD for 2, 4, and 8 weeks [30]. Raw values for these cholesterol levels were used to assess correlations

between blood plasma cholesterol levels and our indices of bone cholesterol content and density.

For our analyses, the left femurs were thawed, cleaned of soft tissues, dried in an oven at 100^{o}C for 2 days, and placed on a scale to measure their dry weight. The dried femur bones were then crushed into powder form using a mortar and pestle and subsequently weighed for their powder weight. This powder was used to measure bone matrix cholesterol content.

Bone Cholesterol Extraction/Quantification

The extraction of cholesterol from the mice femurs was based on the methods of Bligh and Dyer [69]. Cholesterol was extracted from the bone powder of each femur in a solution containing 1.5mL of a 1:2 (v/v) mixture of chloroform and methanol. After a 10 minute incubation with agitation at room temperature, an additional 750 µL of chloroform and 750 µL of water were added to the mixture. This mixture was centrifuged at 1900xG for 10 minutes at room temperature. The top supernatant layer was then aspirated and the remaining alcoholic layer was allowed to completely evaporate at 40-50°C using a water bath. After complete evaporation, the extracted cholesterol was solubilized in 10% triton X-100 in isopropyl-alcohol and stored at -20°C until needed for measurement.

The reconstituted cholesterol for each bone sample was mixed with the color reagent of the Free Cholesterol E kit (Wako) and incubated at 37°C for 5 minutes. A BioTek (µQuant) spectrophotometer was used to measure the absorbance at 600nm. The absorbance readings were fitted to a standard curve according to the manufacturer's instructions to determine the concentration of free cholesterol in each sample.

Results & Discussion

We carried out our analyses to determine if hypercholesterolemia in these animals due to high fat dieting had an influence on body weight, dry bone weight, and bone powder weight as well as blood free cholesterol, blood total cholesterol, and bone free cholesterol levels.

Hypercholesterolemia and Body Weight

As shown in Figure 21, there is a significant difference ($p < 0.05$) in body weight displayed by mice on either HFD or ND for 4 and 8 weeks. This result agrees with previous data [88] considering hypercholesterolemia in these animals have been associated with obesity [89].

Hypercholesterolemia and Femur Dry Weight

A comparison between the dry weights of femurs harvested from mice fed either a HFD or ND is shown in Figure 22. There was no significant difference in dry weights of femurs from mice fed a HFD or ND for all diet durations tested (i.e., up to 8 weeks). Since dry weight is an indicator of the amount of bone mineral content obtained, these data suggested that hypercholesterolemia resulting from high fat dieting for 2, 4, or 8 weeks has no impact on the mineralized weight of bone. Similarly, we did not detect any significant difference in the powder weights of femurs harvested from mice fed either a HFD or ND for up to 8 weeks (Figure 23). It should be noted that hypercholesterolemic diets in mice have not indicated any osteoporotic effects before 8 weeks [14]. Thus,

future investigations are needed that involve mice on hypercholesterolemic diets for more than 8 weeks.

Hypercholesterolemia and Free Bone Cholesterol

The powdered bone was used to measure the free cholesterol levels in HFD and ND mice. A comparison between bone free cholesterol levels for femurs harvested from mice on either HFD or ND is shown in Figure 29. We did not detect any significant difference between bone free cholesterol levels in mice from either HFD or ND for all diet durations tested (Figure 26).

Pearson Analyses to link Blood Cholesterol with Changes in Bone Free Cholesterol Levels

Pearson correlation analyses between all measurements were conducted. The analysis assessed inter-relationships between the following measurements: length of diet, body weight, dry weight, blood free cholesterol, blood total cholesterol, and bone free cholesterol normalized to powder weight. These analyses were conducted in order to determine a link between blood cholesterol levels and bone cholesterol levels in HFD and ND mice.

Based on our analysis shown in Table 5, we only detected significant correlations between diet duration vs. body weight and for bone dry weight vs. bone free cholesterol levels for NFD mice. There was also a link between the diet duration and the body weight in the mice, as expected. Also, the significant difference between dry weight and bone free cholesterol that is normalized to powder weight is due to the fact that the powder

weight is correlated to the dry weight (Table 5). No other correlations were detected for ND mice (Table 5).

There were two significant correlations detected for high-fat diet type mice; length of diet vs. blood total cholesterol, as expected, and blood free cholesterol vs. blood total cholesterol (Table 6). The correlation between total cholesterol and blood free cholesterol agrees with report from previous studies [30]. Notably, we did not detect a significant correlation between bone free cholesterol levels and blood total or free cholesterol levels in HFD mice (Table 6).

It appears from these pilot results that hypercholesterolemic dieting did not cause any changes in the interstitial concentrations of cholesterol in bone for the up to 8-week diet durations tested (Figure 26 & Tables 5-6). These data suggest that the link between hypercholesterolemia and osteoporosis may not, in fact, be explained by the effects of cholesterol elevations in the bone microenvironment on the pressure-sensitive regulation of bone formation by osteoblasts. It should be noted, however, that the accumulated evidence in the literature have not shown hypercholesterolemic dieting to promote osteoporosis in animals for diet durations less than 12 weeks [14]. Thus, in future studies, we plan to conduct additional studies using mice subjected to hypercholesterolemic diets for periods longer than 8 weeks.

Table 4: Total and Free Blood Cholesterol Concentrations of LDLr-deficient Mice. Data indicates mean ± SEM of cholesterol concentrations after 2, 4, and 8 weeks of normal (ND) and high-fat (HFD) diets in LDLr-deficient mice. All data was collected in a previous study [30].

Cholesterol Type	Diet	Cholesterol Concentration (mg/dL)		
		2-week	4-week	8-week
Total	ND	125 ± 11	207 ± 20	281 ± 43
	HFD	642 ± 33	852 ± 72	1215 ± 228
Free	ND	59 ± 3	62 ± 3	71 ± 4
	HFD	289 ± 21	374 ± 26	449 ± 56

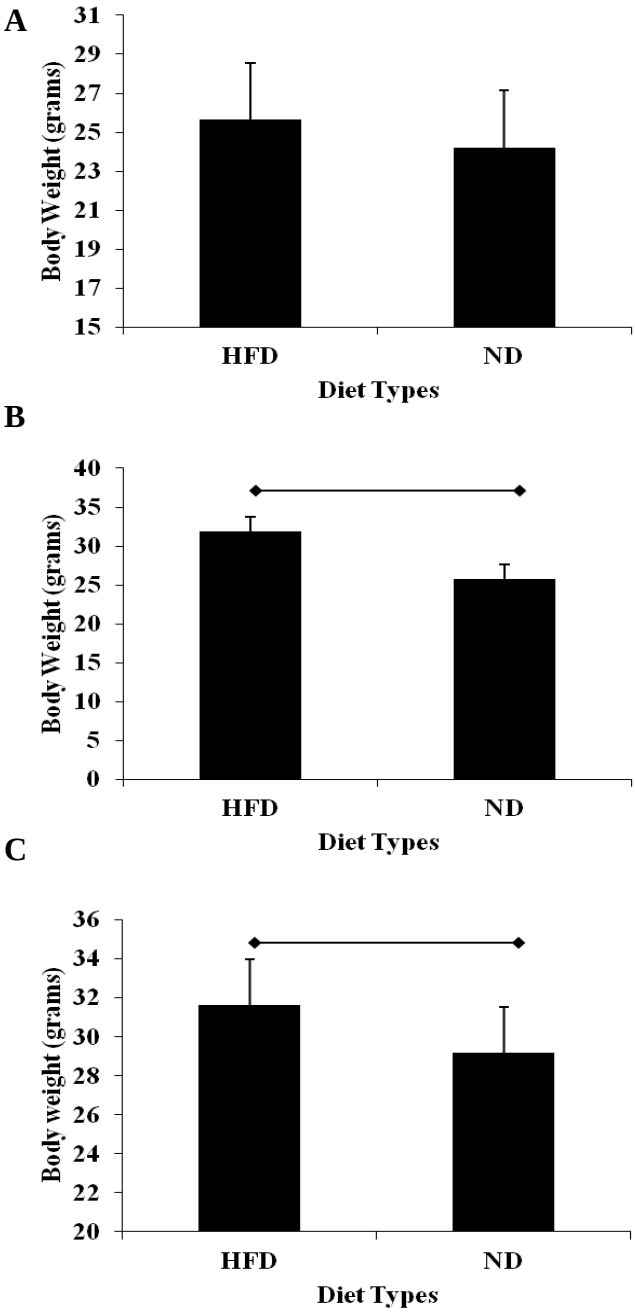

Figure 21: Hypercholesterolemic Diets have an Effect on Body Weight of Mice. Body weight (in grams) is compared between high-fat (HFD) and normal (ND) diets of mice after 2 [Panel A], 4 [Panel B], and 8 [Panel C] weeks. The vertical lines indicate one standard deviation above the average body weight indicated by the bar. Horizontal line indicates a significant ($p<0.01$) difference based on Student's t-test; n=28.

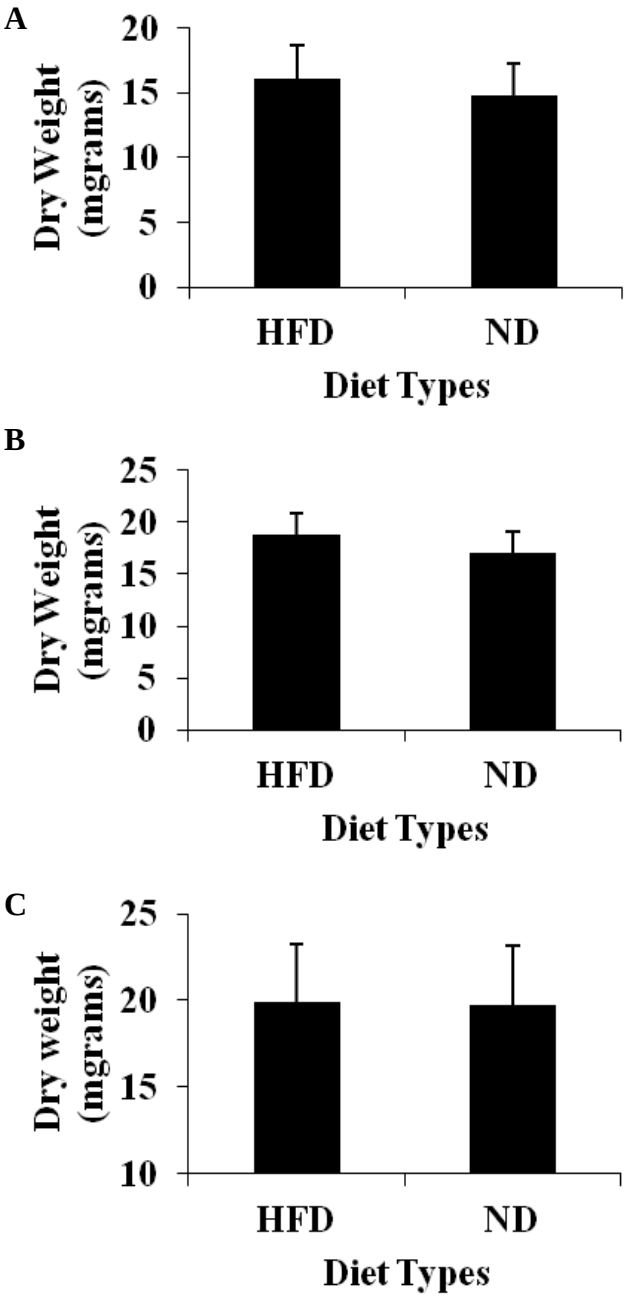

Figure 22: Hypercholesterolemic Diets have no Effect on Dry Bone Weight of Mice. Dry bone weight (in mgrams) is compared between high-fat (HFD) and normal (ND) diets of mice after 2 [Panel A], 4 [Panel B], and 8 [Panel C] weeks. The vertical lines indicate one standard deviation above the average femur dry weight (bars); n=28.

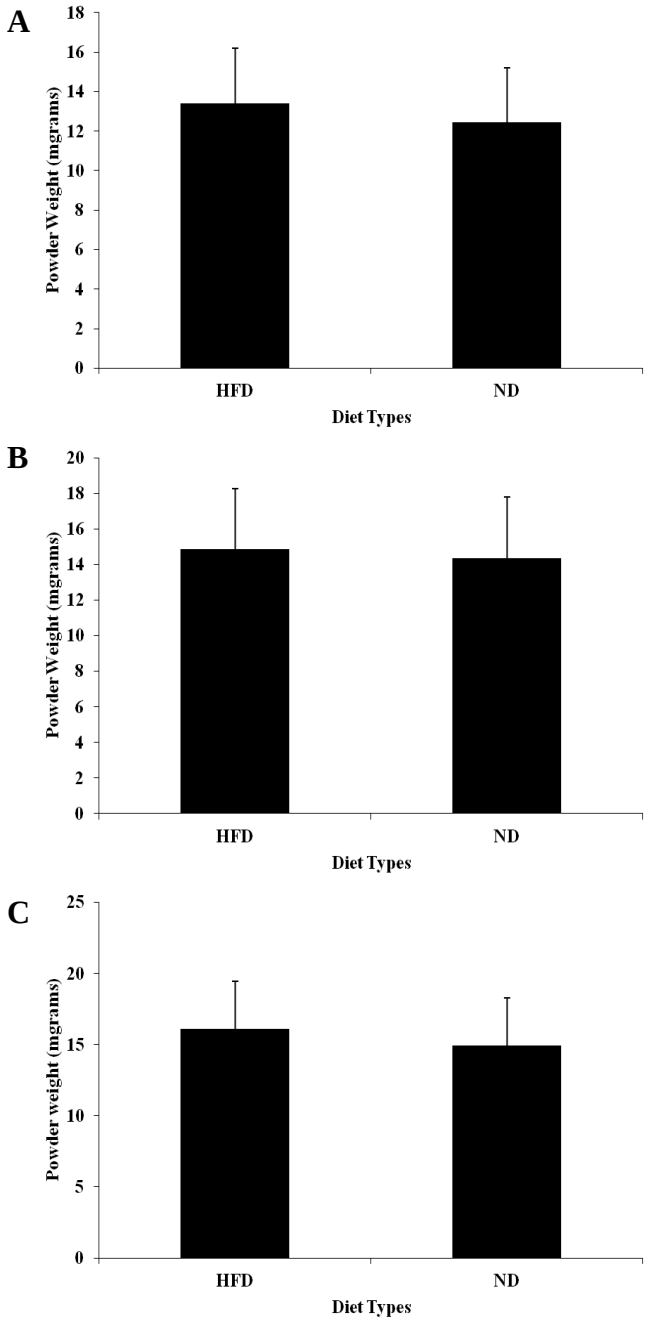

Figure 23: Hypercholesterolemic Diets have no Effect on Powder Bone Weight of Mice. Powder bone weight (in mgrams) is compared between high-fat (HFD) and normal (ND) diets of mice after 2 [Panel A], 4 [Panel B], and 8 [Panel C] weeks. The vertical lines indicate one standard deviation above the average femur powder weight (bar) ; n=28.

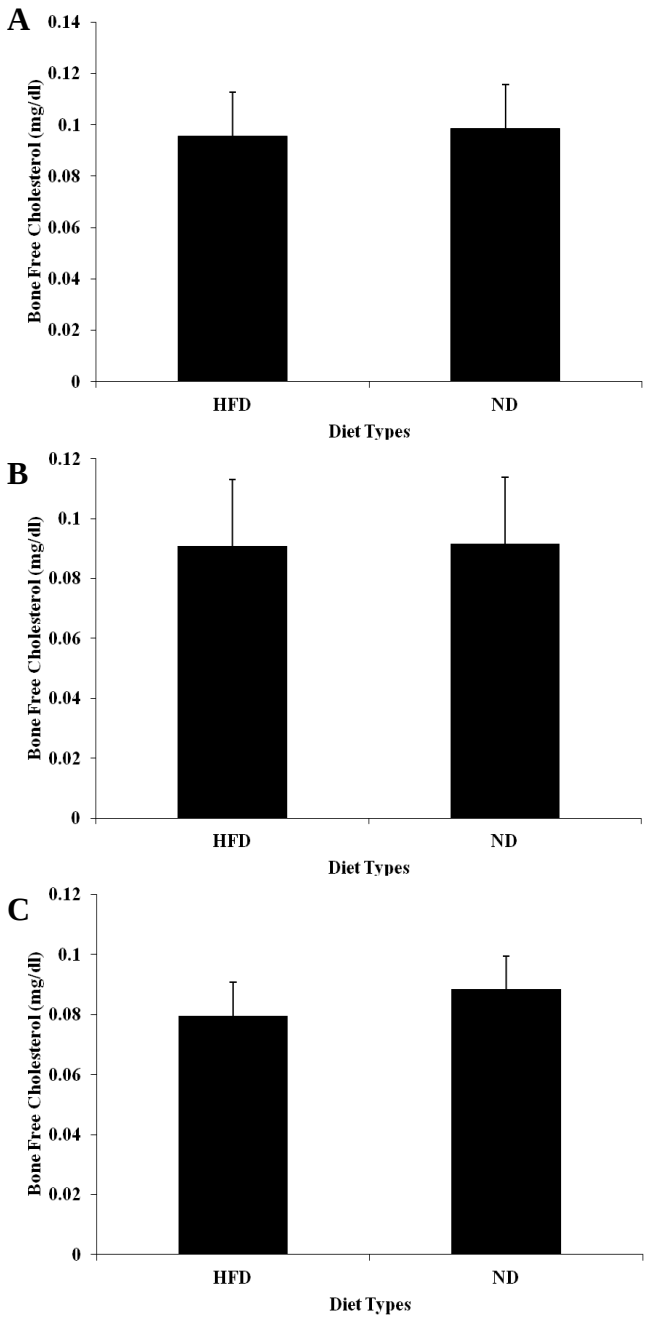

Figure 24: Hypercholesterolemic Diets have no Effect on Bone Free Cholesterol of Mice. Bone free cholesterol (in mg/dL) is compared between high-fat (HFD) and normal (ND) diets of mice after 2 [Panel A], 4 [Panel B], and 8 [Panel C] weeks. The vertical lines indicate one standard deviation above the average values (bars) ; n=28.

Table 5: Normal-Fat Diets Between Length of Diet, Body Weight, Dry Bone Weight, Blood Free Cholesterol, Blood Total Cholesterol, and Bone Free Cholesterol have no Correlation. A correlation analysis depicting a Pearson r-value coefficient (top number) and a two-tailed p-value (bottom number). An asterisk indicates a significant correlation ($p<0.05$); n=14.

		Length of Diet	Body Weight	Dry Weight	Blood Free Cholesterol	Blood Total Cholesterol	Bone Free Cholesterol Normalized to Powder Weight
Length of Diet	Pearson r p (two-tailed)	-	-	-	-	-	-
Body Weight	Pearson r p (two-tailed)	0.857 <0.01 *	-	-	-	-	-
Dry Weight	Pearson r p (two-tailed)	0.439 0.153	0.341 0.277	-	-	-	-
Blood Free Cholesterol	Pearson r p (two-tailed)	-0.177 0.582	0.0704 0.828	-0.281 0.376	-	-	-
Blood Total Cholesterol	Pearson r p (two-tailed)	-0.0648 0.841	-0.039 0.906	-0.039 0.905	0.225 0.482	-	-
Bone Free Cholesterol Normalized to Powder Weight	Pearson r p (two-tailed)	-0.259 0.416	-0.221 0.489	-0.853 <0.01 *	0.242 0.449	0.211 0.51	-

Table 6: High-Fat Diets Between Length of Diet, Body Weight, Dry Bone Weight, Blood Free Cholesterol, Blood Total Cholesterol, and Bone Free Cholesterol have no Correlation. A correlation analysis depicting a Pearson r-value coefficient (top number) and a two-tailed p-value (bottom number). An asterisk indicates a significant correlation ($p<0.05$); n=14.

		Length of Diet	Body Weight	Dry Weight	Blood Free Cholesterol	Blood Total Cholesterol	Bone Free Cholesterol Normalized to Powder Weight
Length of Diet	Pearson r p (two-tailed)	-	-	-	-	-	-
Body Weight	Pearson r p (two-tailed)	0.414 0.18	-	-	-	-	-
Dry Weight	Pearson r p (two-tailed)	0.0753 0.816	0.531 0.0754	-	-	-	-
Blood Free Cholesterol	Pearson r p (two-tailed)	0.488 0.108	0.46 0.132	0.0341 0.916	-	-	-
Blood Total Cholesterol	Pearson r p (two-tailed)	0.634 0.0269 *	0.493 0.103	-0.09 0.78	0.879 <0.01 *	-	-
Bone Free Cholesterol Normalized to Powder Weight	Pearson r p (two-tailed)	-0.261 0.413	-0.3 0.343	-0.456 0.137	-0.449 0.143	-0.374 0.231	-

References

1. Grynpas, M., *New insights into the mechanisms of biomineralization.* Calcif Tissue Int, 2013. **93**(4): p. 297-8.
2. Hodgson, S., et al., *American Association of Clinical Endocrinologists medical guidelines for clinical practice for the prevention and treatment of postmenopausal osteoporosis: 2001 edition, with selected updates for 2003.* Endocrine practice: official journal of the American College of Endocrinology and the American Association of Clinical Endocrinologists, 2003. **9**(6): p. 544.
3. Shulha, J.A., et al., *Assessment of the presence and quality of osteoporosis prevention education among at-risk internal medicine patients.* Consult Pharm, 2014. **29**(1): p. 39-46.
4. Woltman, K. and P.T. den Hoed, *Osteoporosis in patients with a low-energy fracture: 3 years of screening in an osteoporosis outpatient clinic.* J Trauma, 2010. **69**(1): p. 169-73.
5. Cummings, S.R. and L.J. Melton, *Epidemiology and outcomes of osteoporotic fractures.* Lancet, 2002. **359**(9319): p. 1761-7.
6. Ziden, L., C.G. Wenestam, and M. Hansson-Scherman, *A life-breaking event: early experiences of the consequences of a hip fracture for elderly people.* Clin Rehabil, 2008. **22**(9): p. 801-11.
7. Kooij, K.W., et al., *Low bone mineral density in patients with well-suppressed HIV infection is largely explained by body weight, smoking and prior advanced HIV disease.* J Infect Dis, 2014.
8. Zhang, Y.D., et al., *Association of the g.19074G>A genetic variant in the osteoprotegerin gene with bone mineral density in Chinese postmenopausal women.* Genet Mol Res, 2014. **13**(3): p. 6646-6652.
9. Halvarsson, A., E. Franzen, and A. Stahle, *Balance training with multi-task exercises improves fall-related self-efficacy, gait, balance performance and physical function in older adults with osteoporosis: a randomized controlled trial.* Clin Rehabil, 2014.
10. Hoffmanova, I. and M. Andel, *[Osteoporosis and bone alterations in celiac disease in adults]*. Vnitr Lek, 2014. **60**(7-8): p. 601-6.
11. Jackson, R.D., et al., *Calcium plus vitamin D supplementation and the risk of fractures.* N Engl J Med, 2006. **354**(7): p. 669-83.
12. Looker, A.C., et al., *Prevalence of low femoral bone density in older U.S. adults from NHANES III.* J Bone Miner Res, 1997. **12**(11): p. 1761-8.
13. Hirasawa, H., et al., *ApoE gene deficiency enhances the reduction of bone formation induced by a high-fat diet through the stimulation of p53-mediated apoptosis in osteoblastic cells.* J Bone Miner Res, 2007. **22**(7): p. 1020-30.
14. Parhami, F., et al., *Atherogenic high-fat diet reduces bone mineralization in mice.* J Bone Miner Res, 2001. **16**(1): p. 182-8.
15. Turek, J.J., et al., *Oxidized lipid depresses canine growth, immune function, and bone formation.* J Nutr Biochem, 2003. **14**(1): p. 24-31.
16. You, L., et al., *High cholesterol diet increases osteoporosis risk via inhibiting bone formation in rats.* Acta Pharmacol Sin, 2011. **32**(12): p. 1498-504.

17. Tanko, L.B., et al., *Relationship between osteoporosis and cardiovascular disease in postmenopausal women.* J Bone Miner Res, 2005. **20**(11): p. 1912-20.
18. Pasco, J.A., et al., *Statin use, bone mineral density, and fracture risk: Geelong Osteoporosis Study.* Arch Intern Med, 2002. **162**(5): p. 537-40.
19. Zhao, C., et al., *[Effects of statins upon bone mineral density in postmenopausal women with hypercholesterolemia]*. Zhonghua Yi Xue Za Zhi, 2013. **93**(29): p. 2309-11.
20. Gradosova, I., et al., *The role of atorvastatin in bone metabolism in male albino Wistar rats.* Pharmazie, 2011. **66**(8): p. 606-10.
21. Tanriverdi, H.A., A. Barut, and S. Sarikaya, *Statins have additive effects to vertebral bone mineral density in combination with risedronate in hypercholesterolemic postmenopausal women.* Eur J Obstet Gynecol Reprod Biol, 2005. **120**(1): p. 63-8.
22. Ageev, F.T., et al., *[Osteoporosis and arterial stiffness: study of 103 women with mild to moderate risk of cardiovascular disease]*. Kardiologiia, 2013. **53**(6): p. 51-8.
23. Steinberg, D., *Atherogenesis in perspective: hypercholesterolemia and inflammation as partners in crime.* Nat Med, 2002. **8**(11): p. 1211-7.
24. Stokes, K.Y., et al., *Hypercholesterolemia promotes inflammation and microvascular dysfunction: role of nitric oxide and superoxide.* Free Radic Biol Med, 2002. **33**(8): p. 1026-36.
25. Folsom, A.R., *Serum total cholesterol concentrations and awareness, treatment, and control of hypercholesterolemia among US adults.* Circulation, 2003. **108**(21): p. e152; author reply e152.
26. Rubin, J., C. Rubin, and C.R. Jacobs, *Molecular pathways mediating mechanical signaling in bone.* Gene, 2006. **367**: p. 1-16.
27. Migliaccio, S., et al., *Is obesity in women protective against osteoporosis?* Diabetes Metab Syndr Obes, 2011. **4**: p. 273-82.
28. Yesil, Y., et al., *Coexistence of osteoporosis (OP) and coronary artery disease (CAD) in the elderly: it is not just a by chance event.* Arch Gerontol Geriatr, 2012. **54**(3): p. 473-6.
29. Burnett, J.R. and S.D. Vasikaran, *Cardiovascular disease and osteoporosis: is there a link between lipids and bone?* Ann Clin Biochem, 2002. **39**(Pt 3): p. 203-10.
30. Zhang, X., *The influence of membrane cholesterol-related shear stress mechanosensitivity on neutrophil flow behavior*, 2012, University of Kentucky Libraries: Lexington, Ky.
31. Kanis, J.A., et al., *The diagnosis of osteoporosis.* J Bone Miner Res, 1994. **9**(8): p. 1137-41.
32. Huang, M.S., et al., *Hyperlipidemia impairs osteoanabolic effects of PTH.* J Bone Miner Res, 2008. **23**(10): p. 1672-9.
33. Orozco, P., *Atherogenic lipid profile and elevated lipoprotein (a) are associated with lower bone mineral density in early postmenopausal overweight women.* Eur J Epidemiol, 2004. **19**(12): p. 1105-12.

34. Turner, C.H. and F.M. Pavalko, *Mechanotransduction and functional response of the skeleton to physical stress: the mechanisms and mechanics of bone adaptation.* J Orthop Sci, 1998. **3**(6): p. 346-55.
35. Klein-Nulend, J., R.G. Bacabac, and A.D. Bakker, *Mechanical loading and how it affects bone cells: the role of the osteocyte cytoskeleton in maintaining our skeleton.* Eur Cell Mater, 2012. **24**: p. 278-91.
36. Weinbaum, S., S.C. Cowin, and Y. Zeng, *A model for the excitation of osteocytes by mechanical loading-induced bone fluid shear stresses.* J Biomech, 1994. **27**(3): p. 339-60.
37. Chen, J.H., et al., *Boning up on Wolff's Law: mechanical regulation of the cells that make and maintain bone.* J Biomech, 2010. **43**(1): p. 108-18.
38. Gardinier, J.D., et al., *Cyclic Hydraulic Pressure and Fluid Flow Differentially Modulate Cytoskeleton Re-Organization in MC3T3 Osteoblasts.* Cell Mol Bioeng, 2009. **2**(1): p. 133-143.
39. Klein-Nulend, J., et al., *Mechanical loading stimulates the release of transforming growth factor-beta activity by cultured mouse calvariae and periosteal cells.* J Cell Physiol, 1995. **163**(1): p. 115-9.
40. Roelofsen, J., J. Klein-Nulend, and E.H. Burger, *Mechanical stimulation by intermittent hydrostatic compression promotes bone-specific gene expression in vitro.* J Biomech, 1995. **28**(12): p. 1493-503.
41. Thompson, W.R., C.T. Rubin, and J. Rubin, *Mechanical regulation of signaling pathways in bone.* Gene, 2012. **503**(2): p. 179-93.
42. Nagatomi, J., et al., *Frequency- and duration-dependent effects of cyclic pressure on select bone cell functions.* Tissue Eng, 2001. **7**(6): p. 717-28.
43. Henstock, J.R., et al., *Cyclic hydrostatic pressure stimulates enhanced bone development in the foetal chick femur in vitro.* Bone, 2013. **53**(2): p. 468-77.
44. Turner, C.H., *Three rules for bone adaptation to mechanical stimuli.* Bone, 1998. **23**(5): p. 399-407.
45. Li, P., et al., *Fluid flow-induced calcium response in osteoclasts: signaling pathways.* Ann Biomed Eng, 2014. **42**(6): p. 1250-60.
46. Liu, C., et al., *Effects of cyclic hydraulic pressure on osteocytes.* Bone, 2010. **46**(5): p. 1449-56.
47. Burger, E.H., J. Klein-Nulend, and J.P. Veldhuijzen, *Mechanical stress and osteogenesis in vitro.* J Bone Miner Res, 1992. **7 Suppl 2**: p. S397-401.
48. Tanck, E., et al., *Why does intermittent hydrostatic pressure enhance the mineralization process in fetal cartilage?* J Biomech, 1999. **32**(2): p. 153-61.
49. Myers, K.A., et al., *Hydrostatic pressure sensation in cells: integration into the tensegrity model.* Biochem Cell Biol, 2007. **85**(5): p. 543-51.
50. Wu, M.J., Z.Y. Gu, and W. Sun, *Effects of hydrostatic pressure on cytoskeleton and BMP-2, TGF-beta, SOX-9 production in rat temporomandibular synovial fibroblasts.* Osteoarthritis Cartilage, 2008. **16**(1): p. 41-7.
51. Nagatomi, J., et al., *Effects of cyclic pressure on bone marrow cell cultures.* J Biomech Eng, 2002. **124**(3): p. 308-14.
52. Klein-Nulend, J., et al., *Increased bone formation and decreased bone resorption in fetal mouse calvaria as a result of intermittent compressive force in vitro.* Bone Miner, 1987. **2**(6): p. 441-8.

53. Klein-Nulend, J., et al., *Inhibition of osteoclastic bone resorption by mechanical stimulation in vitro.* Arthritis Rheum, 1990. **33**(1): p. 66-72.
54. Nagatomi, J., et al., *Cyclic pressure affects osteoblast functions pertinent to osteogenesis.* Ann Biomed Eng, 2003. **31**(8): p. 917-23.
55. Jacobs, C.R., S. Temiyasathit, and A.B. Castillo, *Osteocyte mechanobiology and pericellular mechanics.* Annu Rev Biomed Eng, 2010. **12**: p. 369-400.
56. Lu, H., et al., *Characterization of ring-like f-actin structure as a mechanical partner for spindle positioning in mitosis.* PLoS One, 2014. **9**(10): p. e102547.
57. Heng, Y.W. and C.G. Koh, *Actin cytoskeleton dynamics and the cell division cycle.* Int J Biochem Cell Biol, 2010. **42**(10): p. 1622-33.
58. Chen, N.X., et al., *Ca(2+) regulates fluid shear-induced cytoskeletal reorganization and gene expression in osteoblasts.* Am J Physiol Cell Physiol, 2000. **278**(5): p. C989-97.
59. Pavalko, F.M., et al., *Fluid shear-induced mechanical signaling in MC3T3-E1 osteoblasts requires cytoskeleton-integrin interactions.* Am J Physiol, 1998. **275**(6 Pt 1): p. C1591-601.
60. Plotkin, L.I. and T. Bellido, *Beyond gap junctions: Connexin43 and bone cell signaling.* Bone, 2013. **52**(1): p. 157-66.
61. Ferraro, J.T., et al., *Depletion of plasma membrane cholesterol dampens hydrostatic pressure and shear stress-induced mechanotransduction pathways in osteoblast cultures.* Am J Physiol Cell Physiol, 2004. **286**(4): p. C831-9.
62. Shin, H.Y., R.M. Underwood, and M.W. Fannon, *Fluid pressure is a magnitude-dependent modulator of early endothelial tubulogenic activity: implications related to a potential tissue-engineering control parameter.* Tissue Eng Part A, 2012. **18**(23-24): p. 2590-600.
63. Underwood, R.M., *The effects of hydrostatic pressure on early endothelial tubulogenic processes*, 2013, University of Kentucky Libraries: Lexington, Ky.
64. Nagatomi, J., et al., *Cyclic pressure affects osteoblast functions pertinent to osteogenesis.* Annals of biomedical engineering, 2003. **31**(8): p. 917-23.
65. Klein-Nulend, J., et al., *Mechanical loading stimulates the release of transforming growth factor-beta activity by cultured mouse calvariae and periosteal cells.* Journal of cellular physiology, 1995. **163**(1): p. 115-9.
66. Klein-Nulend, J., et al., *Increased bone formation and decreased bone resorption in fetal mouse calvaria as a result of intermittent compressive force in vitro.* Bone and mineral, 1987. **2**(6): p. 441-8.
67. Roelofsen, J., J. Klein-Nulend, and E.H. Burger, *Mechanical stimulation by intermittent hydrostatic compression promotes bone-specific gene expression in vitro.* Journal of biomechanics, 1995. **28**(12): p. 1493-503.
68. Nagatomi, J., et al., *Frequency- and duration-dependent effects of cyclic pressure on select bone cell functions.* Tissue engineering, 2001. **7**(6): p. 717-28.
69. Bligh, E.G. and W.J. Dyer, *A rapid method of total lipid extraction and purification.* Can J Biochem Physiol, 1959. **37**(8): p. 911-7.
70. Celedon, G., et al., *Membrane lipid diffusion and band 3 protein changes in human erythrocytes due to acute hypobaric hypoxia.* Am J Physiol, 1998. **275**(6 Pt 1): p. C1429-31.

71. Yan, Y.X., et al., *Mechanical strain regulates osteoblast proliferation through integrin-mediated ERK activation.* PLoS One, 2012. **7**(4): p. e35709.
72. Duncan, R.L. and C.H. Turner, *Mechanotransduction and the functional response of bone to mechanical strain.* Calcif Tissue Int, 1995. **57**(5): p. 344-58.
73. Huang, H., R.D. Kamm, and R.T. Lee, *Cell mechanics and mechanotransduction: pathways, probes, and physiology.* Am J Physiol Cell Physiol, 2004. **287**(1): p. C1-11.
74. Qin, Y.X., W. Lin, and C. Rubin, *The pathway of bone fluid flow as defined by in vivo intramedullary pressure and streaming potential measurements.* Ann Biomed Eng, 2002. **30**(5): p. 693-702.
75. Zhang, D., S. Weinbaum, and S.C. Cowin, *Estimates of the peak pressures in bone pore water.* J Biomech Eng, 1998. **120**(6): p. 697-703.
76. Danion, F., et al., *Stride variability in human gait: the effect of stride frequency and stride length.* Gait Posture, 2003. **18**(1): p. 69-77.
77. Maniotis, A.J., C.S. Chen, and D.E. Ingber, *Demonstration of mechanical connections between integrins, cytoskeletal filaments, and nucleoplasm that stabilize nuclear structure.* Proc Natl Acad Sci U S A, 1997. **94**(3): p. 849-54.
78. Knight, M.M., et al., *Mechanical compression and hydrostatic pressure induce reversible changes in actin cytoskeletal organisation in chondrocytes in agarose.* J Biomech, 2006. **39**(8): p. 1547-51.
79. Burr, D.B., A.G. Robling, and C.H. Turner, *Effects of biomechanical stress on bones in animals.* Bone, 2002. **30**(5): p. 781-6.
80. McBeath, R., et al., *Cell shape, cytoskeletal tension, and RhoA regulate stem cell lineage commitment.* Dev Cell, 2004. **6**(4): p. 483-95.
81. Huang, S. and D.E. Ingber, *The structural and mechanical complexity of cell-growth control.* Nat Cell Biol, 1999. **1**(5): p. E131-8.
82. Hua, V.Y., W.K. Wang, and P.H. Duesberg, *Dominant transformation by mutated human ras genes in vitro requires more than 100 times higher expression than is observed in cancers.* Proc Natl Acad Sci U S A, 1997. **94**(18): p. 9614-9.
83. Kwon, R.Y., et al., *Microfluidic enhancement of intramedullary pressure increases interstitial fluid flow and inhibits bone loss in hindlimb suspended mice.* J Bone Miner Res, 2010. **25**(8): p. 1798-807.
84. Qi, M., et al., *Cholesterol-regulated stress fiber formation.* J Cell Biochem, 2009. **106**(6): p. 1031-40.
85. Thorin, E., et al., *Oxidized-LDL induced changes in membrane physico-chemical properties and [Ca2+]i of bovine aortic endothelial cells. Influence of vitamin E.* Atherosclerosis, 1995. **114**(2): p. 185-95.
86. Pelton, K., et al., *Hypercholesterolemia promotes an osteoporotic phenotype.* Am J Pathol, 2012. **181**(3): p. 928-36.
87. Parhami, F., A. Garfinkel, and L.L. Demer, *Role of lipids in osteoporosis.* Arterioscler Thromb Vasc Biol, 2000. **20**(11): p. 2346-8.
88. Nishina, P.M., J. Verstuyft, and B. Paigen, *Synthetic low and high fat diets for the study of atherosclerosis in the mouse.* J Lipid Res, 1990. **31**(5): p. 859-69.
89. Drolet, M.C., et al., *A high fat/high carbohydrate diet induces aortic valve disease in C57BL/6J mice.* J Am Coll Cardiol, 2006. **47**(4): p. 850-5.

Vita

KRISTEN NICOLE LOUGH

Education

B.S. Mechanical Engineering, Graduated Dec. 2010
University of Kentucky, Lexington, Kentucky

Work Experience

University of Kentucky, Lexington, Kentucky Aug. 2011-present
Graduate Research Assistant,
Cellular Mechanotransduction Laboratory,
Department of Biomedical Engineering

Altec Industries, Elizabethtown, Kentucky May 2010- Aug. 2010
Manufacturing Engineering Co-op

University of Kentucky, Lexington, Kentucky May 2009- May 2010
Undergraduate Research Assistant,
Biomaterials Laboratory,
Department of Biomedical Engineering

University of Kentucky, Lexington, Kentucky May 2008- Aug. 2008
Undergraduate Research Assistant,
Biomechanics Laboratory,
Department of Biomedical Engineering

Target, Dayton, Ohio Sept. 2004- Dec. 2007
Guest Services Team Leader

Awards & Scholarships

National Science Foundation-Kentucky EPSCoR Research Scholars Program Recipient

Graduate Research Assistantship; Biomedical Engineering Department, University of Kentucky, Lexington, Kentucky

Professional Conference Abstracts/Presentations

Lough, K.N. and Shin, H.Y. (2014) "Effects of Membrane Cholesterol Enrichment on Osteoblast Responsiveness to Hydrodynamic" Poster Presentation, *Biomedical Engineering Society: Annual Conference,* San Antonio, Texas.

Lough, K.N. and Shin, H.Y. (2014) "Cholesterol Alters the Osteoblast Mechanosensitivity to Hydrodynamic Pressure Stimulation" Scholar Presentation, *University of Kentucky: Center for Clinical and Translational Science Spring Conference,* Lexington, Kentucky.

Lough, K. N. and Shin, H.Y. (2013) "Exploring the Responsiveness of Osteoblasts to Fluid Pressure Stimulation: A Pilot Study to Examine the Relationship Between Hypercholesterolemia and Osteoporosis" Poster Presentation, *University of Kentucky: Center for Clinical and Translational Science Spring Conference,* Lexington, Kentucky.

Lough, K.N. and Shin, H.Y. (2013) "Influence of Cholesterol on the Responsiveness of Osteoblasts to Fluid Pressure Stimulation" Seminar Presentation, *University of Kentucky: Biomedical Engineering Department*, Lexington, Kentucky.

Professional Memberships & Affiliations

Biomedical Engineering Society (BMES) -
Vice President (2012-2013)
Student member(2008-present)

Alpha Omicron Pi Sorority -
Christmas for the Kids Charity Chair (2009),
Executive Recruitment Committee (2008-2009)
Social Chair Assistant (2007-2008)

Society of Women Engineers (SWE) -
Student member(2006-present)

American Institute of Aeronautics and Astronautics (AIAA) -
Student member (2008-2010)

Order of Engineers -
Member(2010-present)